Influence of initial soil moisture in a Regional Climate Model study over West Africa. Part 2: Impact on the climate extremes

Brahima KONÉ[1], Arona DIEDHIOU[1, 2], Adama Diawara[1], Sandrine Anquetin[2], N'datchoh Evelyne Touré[1], Adama Bamba[1] and Arsene Toka Kobea[1]

[1]LASMES - African Centre of Excellence on Climate Change, Biodiversity and Sustainable Agriculture (ACE CCBAD) / Université Félix Houphouët Boigny, Abidjan, Côte d'Ivoire

[2]Univ. Grenoble Alpes, IRD, CNRS, Grenoble INP, IGE, F-38000 Grenoble, France

Correspondence to: Arona DIEDHIOU (arona.diedhiou@ird.fr)

Abstract.
The influence of the soil moisture initial conditions on climate extreme indices over West Africa is investigated using the fourth generation of Regional Climate Model version 4 (non-hydrostatic) coupled to the version 4.5 of the Community Land Model (RegCM4-CLM4.5) at 25 km spatial resolution. We initialized the control experiments with the reanalysis soil moisture of the European Centre Meteorological Weather Forecast's reanalysis of the 20th century data (ERA20C), while for the dry and wet experiments, we initialized the soil moisture at the maximum and minimum value over West Africa domain, respectively. For each experiment, an ensemble of five runs are performed for five years (2001- 2005), with soil moisture initial conditions prescribed on June 1 and simulations performed over four months (122 days) from June to September. The performance of RegCM4-CLM4.5 in simulating the ten extreme rainfall and temperature indices used in this study is presented. Then, the results are discussed for the two idealized simulations most sensitive to the dry and wet soil moisture initial conditions to highlight the impacts beyond the limits of soil moisture internal forcing in the model. Over the Central Sahel, dry (wet) experiments lead to a decrease (increase) of precipitation extreme indices related to the number of events, not for those related to the intensity of the events. Soil moisture initial conditions unequally affect the daily minimum and maximum temperatures. The strongest impact is found on the maximum temperature. Wet (dry)

32 experiments decrease (increase) maximum temperature in the whole region. Over the Central

33 Sahel, wet (dry) experiments lead to a decrease (increase) of the maximum values of minimum

34 temperature.

1 Introduction

37 West Africa experienced large rainfall variability during the late 1960s. This variability often

38 leads to flooding events, severe drought, and regional heatwaves, which have major economic,

39 environmental, and societal impacts (Easterling et al., 2000; Larsen, 2003). In recent years,

40 climate extremes have attracted much interest because they are expected to occur more

41 frequently (International Panel on Climate Change (IPCC), 2012) than changes in the mean

42 climate. Yan and Yang (2000) showed that for many cases, the extreme climate changes were

43 five to ten times greater than climate mean change. Many key factors or physical mechanisms

44 could be the cause of the increase in climate extremes (Nicholson, 1980; Le Barbé et al., 2002),

45 such as the effect of increasing greenhouse gases in the atmosphere on the intensification of hot

46 extremes (IPCC, 2007), sea surface temperature (SST) anomalies (Fontaine and Janicot 1996;

47 Folland et al., 1986), and land surface conditions (Philippon et al., 2005; Nicholson (2000)). In

48 addition, smaller-scale physical processes, including the interactions of land–atmosphere

49 coupling, can lead to changes in climate extremes. For the European summer, the influence of

50 soil moisture on land–atmosphere coupling using a regional climate model and focused on the

51 extremes and trends in precipitation and temperature have been studied by Jaeger and

52 Seneviratne (2011). For extreme temperatures, their studies have shown that interactions of soil

53 moisture and climate have a significant impact, while for extreme precipitation, they only

54 influence the frequency of wet days. Over Asia, Liu et al. (2014) studied the impact on

55 subsequent precipitation and temperature of soil moisture anomalies using a regional climate

56 model. They showed that wet (dry) experiences decrease (increase) the hot extremes, decrease

57 (increase) the drought extremes, and increase (decrease) the cold extremes in a zone with strong

58 soil moisture–atmospheric coupling. However, none of these studies examined the impacts of

59 the soil moisture initial conditions on subsequent climate extremes using a regional climate

60 model over West Africa. In part 1, the influence of initial soil moisture on the climate mean

61 was based on a performance assessment of the Regional Climate Model coupled with the

62 complex Community Land Model (RegCM4-CLM4.5) performed by Koné et al. (2018), where

63 the ability of the model to reproduce the climate mean has been validated. However, in Part 2,

before starting to study the influence of initial soil moisture on climate extremes, it was necessary to assess the performance of RegCM4-CLM4.5 in simulating the ten temperature indices and extreme rainfall events used in this study. This has never been done before in Africa; therefore, we separated the work in two parts. The manuscript is organized as follows: Section 2 describes the RegCM4 model, experimental design, and methodology used in this study; Section 3 presents the assessment of RegCM4-CLM4.5 in extreme climate simulation and the impacts on climate extremes of the soil moisture initial conditions; and Section 4 documents the conclusions.

2. Model, experimental design and methodology

2.1 Model description and numerical experiments

The fourth generation of the Regional Climate Model (RegCM4) of the International Centre for Theoretical Physics (ICTP) is used in this study. Since this version, physical representations have been subject to a continuous process of implementation and development. The release used in this study was RegCM4.7. The non-hydrostatic dynamical core of the MM5 (Mesoscale Model version 5, Grell et al., 1994) was ported to RegCM4 while maintaining the existing hydrostatic core. RegCM4 is a limited-area model using a vertical grid sigma hydrostatic pressure coordinate and a horizontal grid of the Arakawa B-grid (Giorgi et al., 2012). The radiation scheme is from the NCAR-CCM3 (National Center for Atmospheric Research and the Community Climate Model Version 3) (Kiehl et al., 1996), and the aerosol representation is from Zakey et al. (2006) and Solmon et al. (2006). The large-scale precipitation scheme used in this study is from Pal et al. (2000); the moisture scheme is called the SUBgrid EXplicit moisture scheme (SUBEX), which considers the sub-grid variability in clouds. The accretion and evaporation processes for stable precipitation are from Sundqvist et al. (1989). The sensible heat and water vapour in the planetary boundary layer over land and ocean, as well as the turbulent transport of momentum, is reported by Holtslag et al. (1990). The heat and moisture and momentum of ocean surface fluxes are from Zeng et al. (1998). Convective precipitation and land surface processes in RegCM4.7 are represented in several options. Based on Koné et al. (2018), the convective scheme of Emanuel (1991) is used. The parameterization of land surface processes is from CLM4.5 (Oleson et al., 2013). In each grid cell of CLM4.5, there are sixteen different plant functional types and ten soil layers (Lawrence et al., 2011; Wang et al., 2016). The integration of RegCM4 over the West African domain is shown in Fig. 1 with eighteen vertical levels and 25 km of horizontal resolution (182 × 114 grid points; from 20°W

96 - 20°E and 5°S - 21°N). The European Centre for Medium-Range Weather Forecasts reanalysis

97 (EIN75; Uppala et al., 2008; Simmons et al., 2007) provides the initial and boundary conditions.

98 The sea surface temperatures (SSTs) are derived from the National Oceanic and Atmosphere

99 Administration optimal interpolation weekly (NOAA; OI_WK) (Reynolds et al., 1996). The

100 topography is derived from the United States Geological Survey (USGS) Global Multi-

101 resolution Terrain Elevation Data (GMTED; Danielson et al., 2011) at a spatial resolution of

102 30 arc-s, which is an update of the Global Land Cover Characterization (GTOPO; Loveland et

103 al., 2000) dataset.

104 We used the soil moisture from the reanalysis of the European Centre Meteorological Weather

105 Forecast's Reanalysis of the 20th century (ERA20C) to initialize the control runs. Wet and dry

106 experiments were initialized for the soil moisture at the maximum (= 0.489 $m^3.m^{-3}$) and

107 minimum (= $0.117.10^{-4}$ $m^3.m^{-3}$) soil moisture values over West Africa derived from the

108 ERA20C soil moisture dataset. We designed three experiments (reference, wet, and dry), each

109 with an ensemble of five (5) simulations (2001, 2002, 2003, 2004, and 2005) starting from June

110 1st to September 30th. The difference between these three experiments is the change in the

111 initial soil moisture condition (reference initial soil moisture condition, wet initial soil moisture

112 condition, and dry initial soil moisture condition) during the first day of the simulation over the

113 West African domain. Then, we selected the two years most affected by the wet and dry initial

114 soil moisture conditions (2003 and 2004) to estimate the limits of the impact of the internal soil

115 moisture forcing on the new non-hydrostatic dynamic core of RegCM4.

116 For these two years most sensitive to soil moisture initial conditions, the Student t-test is used

117 to compare the significance of changes in climate extreme indices between a wet or dry

118 sensitivity test (sample 1) and the control (sample 2) in assuming that this method performs

119 well for climate simulations (Damien et al., 2014) and knowing that it is extensively used for

120 climatological analysis (Menedez et al., 2019; Talahashi and Polcher, 2019). In this study, the t-test

121 at the 95% confidence level was used to consider statistically significant.

122

2.2 Validation datasets and evaluation metrics

124 Our investigation focused on the air temperature at 2 m and the precipitation over the West

125 African domain during JJAS for 2003 and 2004. The simulated precipitation fields are validated

126 with the Climate Hazards Group Infrared Precipitation Stations (CHIRPS) dataset from the

127 University of California at Santa Barbara, available from 1981 to 2020 with 0.05° high-

128 resolution data. We have chosen CHIRPS as reference in this study, mainly because this

129 product has been widely assessed and used for the study of extreme events in West Africa by

130 Bichet et al. (2018a, b) and Didi et al. (2020).

131 We validated the 2-m temperature using the The National Oceanic and Atmospheric

132 Administration (NOAA) Climate Prediction Center (CPC) daily maximum and minimum

133 global surface air temperature. The NOAA/CPC global daily surface 2-m air temperature (CPC-

134 T2m) is a land-only gridded global daily maximum (Tmax) and minimum (Tmin) temperature

135 analysis from 1979 to the present, available at two spatial of 10 min × 10 min and 0.5° × 0.5°

136 (latitude × longitude). This product provides an observational T2m estimate for climate

137 monitoring, model evaluation, and forecast verification (Fan Y. and Huug van den Dool, 2008;

138 Pan et al., 2019). In this study, the daily Tmax and Tmin are used at spatial resolution 0.5° ×

139 0.5°. To compare the model simulations with the observation datasets, we re-gridded all the

140 products to 0.22° × 0.22° using a bilinear interpolation method (Nikulin et al., 2012).

141 The performance of RegCM4-CLM4.5 to simulate the extreme indices is evaluated using four

142 selected sub-regions (Fig. 1) based on the previous work of Koné et al. (2018), which

143 correspond to different annual precipitation cycle features. We used the mean bias (MB), which

144 captures the small-scale differences between the simulation and observation. The pattern

145 correlation coefficient (PCC) is also used as a spatial correlation between model simulations

146 and observations to indicate the large-scale similarity degree.

147 To quantify the impact of soil moisture initial conditions on climate extremes over Asia, Liu et

148 al. (2014) used the MBs in five subregions. In our study, we used the MBs and the probability

149 density functions (PDF, Gao et al. (2016); Jaeger and Seneviratne (2011)) for this purpose to

150 better capture how many grid points are impacted by initial soil moisture and their highest value.

151

2.3. Extreme rainfall and temperature indices

153 In this study, we investigated the changes in precipitation and temperature in terms of duration,

154 occurrence, and intensity of six extreme rainfall and four extreme temperature indices using

155 daily rainfall and daily minimum and maximum temperature data (Table 1). These ten extreme

156 indices are recommended by the Expert Team on Climate Change Detection and Indices

157 (ETCCDI, Peterson et al., 2001).

3. Results and discussion

3.1. Seasonal extreme rainfall

In this section, we analyzed six extreme rainfall indices based on daily precipitation in RegCM4 simulations over West Africa. All precipitation indices were calculated for JJAS in 2003 and 2004. Table 2 summarizes the PCC and the MB of all precipitation indices studied in this section for simulations obtained from control experiments with respect to CHIRPS observations, calculated for the West Sahel, Central Sahel, Guinea Coast, and the entire West African domain during the runs JJAS 2003 and JJAS 2004

3.1.1 The number of the wet days (R1mm)

Figure 2 shows the mean values of the number of wet days (R1mm, in days) from CHIRPS (Fig. 2a, c) observation and the simulated control experiments (Fig. 2b, d) with the initial soil moisture derived from ERA20C reanalysis. The R1mm index maximum values up to 100 days in CHIRPS observation are found over mountainous regions such as the Cameroon Mountains, Jos Plateau, and Guinea Highlands, while minimum values less than 50 days are found over the Sahel and along the coastline from Liberia to Ghana with the number of wet days decreasing gradually from south to north.

The control experiments (Fig. 2b, d) reproduce well the large-scale pattern of the observed rainfall, with PCC values of 0.96 and 0.95 for runs JJAS 2003 and JJAS 2004, respectively (Table 2) over the entire West African domain, but exhibit some spatial extent and magnitude biases at local scale. The control experiments display a large and quite homogeneous area of maximum values of R1mm index below 12 °N latitude and overestimate the number of wet days over most of the studied domains (Table 2). The largest MBs are found over the Guinea Coast with MB values more than 53.16 and 55.46 days for the runs JJAS 2003 and JJAS 2004, respectively (Table 2). This overestimation of the number of wet days in RegCM4 is also found by Thanh et al. (2017) with RegCM4 for Asia.

Figure 2 (second panel) displays additional changes in the R1mm index for JJAS 2003 and JJAS 2004 from the dry (Fig. 2e and g) and wet experiments (Fig. 2f and h) compared to the control experiments; the dotted area shows changes with statistical significance at the 95% level. The dry experiments (Fig. 2e, g) decrease the R1mm index values, while the wet experiments (Fig. 2h, j) increase them, especially over Central Sahel. However, over the Guinea Coast sub-region, both wet and dry experiments show a significant increase in R1mm index values.

191 For a better quantitative evaluation, Figure 3 displays the PDF distributions of changes in

192 R1mm over the sub-domains (Fig. 1), during the runs JJAS 2003 and JJAS 2004 while Table 3

193 summarizes the PDF maximum values. The results essentially confirm the linear impact found

194 over Central Sahel (Fig. 3a). Over West Sahel, the Guinea Coast, and the West African domain

195 (Fig. 3b, c, and d), both dry and wet experiments increase the R1mm index values. The strongest

196 R1mm increase is found in wet experiments over West Sahel, with a maximum change about

197 12 days in JJAS 2003 (Table 3) while the strongest R1mm decrease is found for dry experiments

198 over Central Sahel, with a maximum change about -5.19 days (Table 3).

199 .

200 Summarizing the results of this section, RegCM4 overestimated the number of wet days over

201 most of the studied domains. Over the Central Sahel, wet and dry experiments lead both to a

202 linear impact on the R1mm index with an increase and a decrease respectively of the number

203 of rainy days. These results are compatible with previous work that sustained a strong land–

204 atmosphere coupling in transition areas between wet and dry climate regimes (Zhang et al.,

205 2011; Koster et al., 2006).

206

207 **3.1.2 Simple daily intensity index (SDII).**

208 We analyzed in this section the SDII index (rainfall intensity in mm.day^{-1}) which gives the

209 amount of precipitation mean on total wet days (daily precipitation >1mm). Figure 4 (first

210 panel) is the same as figure 2 (first panel) but for the rainfall intensity. Over the coastline of

211 Guinea Coast, CHIRPS observation (Fig.4a, c) depicted the highest values of SDII index, more

212 than 25 mm.day^{-1}. While, over the Sahel and Sahara, CHIRPS observation showed large extend

213 SDII index values not exceeding 12 mm.day^{-1} in both runs JJAS 2003 and JJAS 2004.

214 The control experiments (Fig. 4 b, d) reproduced well the large-scale pattern of CHIRPS with

215 PCC values reaching 0.73 and 0.77 (in the runs JJAS 2003 and JJAS 2004, respectively; Table

216 2) over the West African domain. However, at the local scale, some biases are found. Over most

217 of the studied domains, the magnitude of the SDII is underestimated and not exceed 10 mm.day^{-}

218 ^{1}, excepted over the Cameroon Mountains (Fig. 4b, d). The largest MB values were located

219 over the Guinea Coast with MB values greater than -13.62 and -14.65 mm.day^{-1} for the runs

220 JJAS 2003 and JJAS 2004, respectively (Table 2).

221 Figure 4 (second panel) is the same as figure 2 (second panel) but for the rainfall intensity.

222 Unlike the R1mm index, changes in the SDII index due to soil moisture initial conditions are

223 not linear over most of studied domains. Fig. 4 (second panel) shows that generally, the impact

224 on rainfall intensity of dry and wet experiments presents areas of increase and decrease over

225 most of the studied sub-domains.

226 Figure 5 displays PDFs of changes in SDII, as in Fig. 3. The PDFs show a maximum change

227 value centered approximately on zero (Table 3), indicating that changes in the rainfall intensity

228 for wet and dry experiments are not significant.

229 In summary, RegCM4 underestimates the rainfall intensity over the studied domain compared

230 to the observation and the impact on SDII index in wet and dry experiments are not significant.

231

232 **3.1.3 Maximum number of consecutive dry days (CDD).**

233 The duration of consecutive dry days (CDD, in days), which represents the maximum number

234 of consecutive dry days with precipitation less than 1 mm.day^{-1} is analyzed in this subsection.

235 Figure 6 (first panel) is the same as figure 2 (first panel) but for CDD. CHIRPS observation

236 locates the highest CDD values over the Sahara, with length more than 50 days (Fig. 6a, c). The

237 lowest CDD values are found over the Guinea Coast, with length less than 8 days.

238 The control experiments (Fig. 6b, d) over the entire West African domain well reproduce the

239 large-scale pattern of the observed rainfall with a PCC values more than 0.85 and 0.89 for the

240 runs JJAS 2003 and JJAS 2004, respectively (Table 1). However, in terms of magnitude, some

241 differences are observed at local scale. In general, the control experiments overestimate the

242 CDD over most of studied subdomains, except over the Guinea Coast (Table 2). The strongest

243 overestimation is found over West Sahel with MB values reaching more than 14.49 and 17.51

244 days for runs JJAS 2003 and JJAS 2004, respectively (Table 2). The current model

245 parameterization increases the drought extreme over most of the studied domains, except over

246 the Guinea Coast (Table 2).

247 Figure 6 (second panel) is the same as figure 2 (second panel) but for CDD. The soil moisture

248 initial condition impact on CDD index is linear over the Central and West Sahel (Fig. 6, second

249 panel); Over the Sahel, dry (wet) experiments increase (decrease) the length of dry spells. Over

250 the Guinea Coast, the impacts on CDD are weak for both dry and wet experiments and in

251 average, soil moisture initial conditions seem to decrease the length of dry spells in a central

252 band between Côte d'Ivoire and Nigeria.

253 Figure 7 is the same as figure 3 but displays the PDF distribution of the changes in CDD. The

254 highest length of CDD increase are found over the Central Sahel in dry experiments with

255 maximum change in length reaching 3.80 days in JJAS 2004 (Table 3), while the highest CDD

256   decrease are found over West Sahel in wet experiments with maximum change in length

257   reaching -12.73 days in the run JJAS 2003 (Table 3).

258   In summary, RegCM4 overestimated the maximum number of consecutive dry days over most

259   studied subdomains, except over the Guinea Coast. However, the impact of soil moisture initial

260   condition is linear over the Central and West Sahel. Over the Guinea Coast, the dry and wet

261   experiments generally decrease the length of dry spells.

262

3.1.4 Maximum number of consecutive wet days (CWD).

264   The duration of wet spells (CWD) which represents the maximum number of consecutive wet

265   days with precipitation ≥ 1 mm.day^{-1} is investigated in this subsection. Figure 8 (first panel) is

266   the same as figure 2 (first panel) but shows the CWD duration. In the CHIRPS observation, the

267   maximum length of CWD lasting longer than 20 days are found over the mountain regions such

268   as Cameroon Mountains, Jos plateau and Guinea highlands. While the minimum length of

269   CWD lasting less than 4 days are found over most of the area above the latitude 17°N (Fig.8a,

270   c).

271   The control experiments well reproduce the large-scale pattern over the entire West African

272   domain, with PCC values around 0.81 and 0.87 (resp. for JJAS 2003 and JJAS 2004, Table 2).

273   However, at local scale, the control experiments exhibit some biases in the CWD minimum and

274   maximum values, both in terms of magnitude and spatial extent. Control experiments

275   overestimate the CWD length over most of subdomains studied (Fig. 8 b, d). We noted that,

276   areas of overestimation coincide with areas of excessive R1mm values (Fig.2b, d). The

277   strongest overestimation is found over the Guinea Coast, reaching 59.21 and 60.51 days (resp.

278   for JJAS 2003 and JJAS 2004, Table 2).

279   Figure 8 (second panel) is the same as figure 2 (second panel), but displays changes in CWD.

280   As for R1mm index, over the Central Sahel, the dry (wet) experiments decrease (increase) CWD

281   length for both JJAS 2003 and JJAS 2004. This result confirms the strong influence of soil

282   moisture initial conditions in the Sahel band, as found by Zhang et al. (201) and Koster et al.

283   (2006) over the transition zones with a climate between dry and wet regimes. However, over

284   Guinea and the West Sahel, the changes are not linear, both dry and wet experiments increase

285   the CWD length (Fig. 8e-h).

286   Figure 9, as in figure 3, but shows the PDF distribution of changes in CWD. The strongest

287   CWD increase is found over Central Sahel with maximum changes reaching 15.58 days in wet

288 experiments, while in dry experiments, the strongest CWD decrease is found in the same sub-
289 domain with maximum changes reaching −4.48 days.

290 Summarizing the results of this section, as for R1mm and CDD indices, the impact of wet and
291 dry experiment on CWD is linear over the Central Sahel meaning that dry (wet) experiments
292 decrease (increase) the CWD lengths. The model RegCM4 overestimates the duration of wet
293 consecutive days over most of studied subdomains. This overestimation is associated with the
294 excessive number of wet days in the model as documented by Diaconescu et al. (2014).

295

296 **3.1.5 Maximum one-day precipitation accumulation (RX1day).**

297 The maximum one-day precipitation accumulation (RX1day) during JJAS 2003 and JJAS 2004
298 is assessed in this section. Figure 10 (first panel) shows the spatial distribution of RX1day.
299 CHIRPS observation confines the spatial extent of RX1day maximum values greater than 80
300 mm over the coastline of the Guinea Coast. While, the large extent of RX1day minimum values
301 less than 50 mm are found over the Sahara, Sahel and part of Guinea Coast.

302 The control experiments capture the spatial pattern of RX1day with PCC values around 0.50
303 and 0.4 for JJAS 2003 and JJAS 2004, respectively (Table 2). This low coefficient of PCC is
304 also obtained by Thanh et al. (2017) over Asia with RegCM4 (correlation < 0.3). The model
305 simulations fail to capture the magnitude and spatial extent of the RX1day maxima. The control
306 experiments underestimate the RX1day over most of studied subdomains and this seems to be
307 associated with the excessive number of weak precipitation simulated by the model. The largest
308 underestimation is located over the Guinea Coast and the West Sahel. For instance, over the
309 West Sahel, the MB values are −38.07 and −36.67 mm for JJAS 2003 and JJAS 2004,
310 respectively (Table 2).

311 Figure 10 (second panel) is similar to Figure 2 (second panel), but displays changes in the
312 RX1day. As for the SDII, the impact of the soil moisture initial conditions on RX1day is not
313 linear (Fig. 10, second panel).

314 Figure 11 is similar to figure 3, but shows the PDF distribution of changes in the RX1day.
315 Increases of RX1day for both dry and wet experiments are found over most of studied
316 subdomains (Fig.11). The strongest increase in RX1day is found over Guinea Coast for wet
317 experiments, with values reaching 26.14 and 14.93 during JJAS 2003 and JJAS 2004,
318 respectively (Table 3).

319 In summary, RegCM4 underestimates the maximum one-day precipitation accumulation over
320 most of studied domain. Both wet and dry experiments lead to an increase of RX1day.

321

3.1.6 Precipitation percent due to very heavy precipitation days (R95pTOT)

In this section, we investigated the precipitation percentage due to very heavy precipitation days during JJAS 2003 and JJAS 2004. Figure 12 (first panel) is the same as figure 2 (first panel), but shows the spatial distribution of R95pTOT. CHIRPS observation confines the R95pTOT maximum values greater than 40% over the Guinea Coast. While R95pTOT index minimum values less than 30 % are found over the Central and West Sahel (Fig. 10 a, c). The control experiments (Fig. 12b, d) capture the large spatial pattern with PCC values of 0.59 and 0.55 for JJAS 2003 and JJAS 2004, respectively (Table 2). As with SDII and RX1day indices, the control experiments underestimate the values of the R95pTOT index, while they overestimate the R1mm index. This is also due to the current physical parameterization scheme of the RegCM4 model, which results in a positive bias for the number of wet days with a low precipitation amount (e.g., 1 mm.day^{-1}), and a negative bias in the number of wet days with a higher precipitation threshold (e.g., 10 mm.day^{-1}, not showed here).

The control experiments underestimate R95pTOT over the different studied domains. The highest R95pTOT underestimation is found over the Guinea Coast with MB values more than −43.22 and −46.61 % for JJAS 2003 and JJAS 2004, respectively (Table 2).

Figure 12 (second panel) is similar to figure 2 (second panel), but displays changes in the R95pTOT index. Both dry and wet experiments lead to R95pTOT index increase over the orographic regions. Therefore, the soil moisture initial conditions, whether dry or wet extreme reinforce occurrence of extreme floods events.

Figure 13 is the same as figure 3 but shows the PDF distribution of changes in the R95pTOT. The highest R95pTOT increase is found over the West Sahel and Guinea Coast with maximum change values around 4.03% and 4.33% for JJAS 2003 and JJAS 2004, respectively (Table 3). In summary, RegCM4 underestimates R95pTOT while the soil moisture initial conditions, whether dry or wet, increase the precipitation percent due to very heavy precipitation days. This result is consistent with Liu et al. (2014) work over Asia using RegCM4.

348

3.2. Temperature extreme indices

In this section, using daily maximum and minimum temperatures, we analyzed four extreme temperature indices (Table 1) in RegCM4 simulations over West Africa. All temperature indices are calculated for JJAS 2003 and JJAS 2004. Table 4 summarizes the PCC and MB of

353 all temperature indices for the control experiments with initial soil moisture from ERA20C
354 reanalysis, with respect to CPC-T2m observation, calculated over the subdomains presented in
355 Fig. 1, during the JJAS 2003 and JJAS 2004.
356

3.2.1. Maximum value of daily maximum temperature (TXx)

358 In this section, we analyzed the TXx, which gives the hottest day's temperature during JJAS
359 2003 and JJAS 2004. Figure 14 (first panel) shows the TXx (in °C) from CPC-T2m observation
360 (Fig. 14a, c) for JJAS 2003 and JJAS 2004 and from the mean control experiments (Fig. 14b,
361 d). The CPC-T2m observation shows that the highest TXx values more than 46 °C are found
362 over the Sahara. The lowest TXx index values less than 32 °C are found over the Guinea Coast
363 (Fig. 14a, d). CPC-T2m observation (Fig. 14a, c) shows the lowest TXx values less than 28 °C
364 along the coastline of the Guinea Coast, while the TXx highest values more than 40 °C are
365 found over Sahara and the northern of Sahel (Fig.14a, c),
366 The control experiments (Fig. 14c, f) reasonably replicate the large-scale patterns of the TXx
367 values with PCCs up to 0.99 (Table 3) over the entire West African domain; however, they
368 exhibit some biases at local scale. The control experiments are closer to the maximum and
369 minimum values displayed in the CPC-T2m observation. The control simulations overestimate
370 the TXx values over the Central and West Sahel, and underestimate them over the Guinea Coast
371 (Table 4). The greatest overestimation is found over the West Sahel with MB values around
372 3.02 and 2.02 °C for JJAS 2003 and JJAS 2004, respectively (Table 4). However, the biases
373 obtained for TXx are much lower than those obtained by Thanh et al. (2017), who used
374 RegCM4 over Asia where they reached 8 °C.
375 Figure 14 (second panel) displays changes in TXx for JJAS 2003 and JJAS 2004 in dry (Fig.
376 14g, i) and wet experiments (Fig. 14h, j) with respect to the control experiments; the dotted area
377 showed significant changes with a statistical significance of 95%. Dry experiments lead to an
378 increase of TXx values, while the wet experiments decrease them.
379 The PDF distributions of TXx changes for JJAS 2003 and JJAS 2004 over (a) the Central Sahel,
380 (b) West Sahel, (c) Guinea Coast, and (d) West Africa derived from dry and wet experiments
381 compared to the control experiments are shown in Fig. 15. Table 5 summarizes the maximum
382 values of changes obtained on the PDF of TXx. The strongest decrease (increase) in the TXx
383 index are found over the Central Sahel with a maximum change around −2.57 °C (more than
384 1.69 °C) in wet (dry) experiments in JJAS 2004.

385   In summary, during JJAS 2003 and JJAS 2004, the RegCM4 model overestimates and
386   underestimates the hottest day's temperature over the Sahel and Guinea Coast, respectively.
387   Dry experiments result in an increase of TXx, while the wet experiments lead to a decrease of
388   TXx values.

389

390   **3.2.2. Minimum value of daily maximum temperature (TXn).**
391   In this section, we investigated the TXn index which gives the lowest day's temperature during
392   JJAS 2003 and JJAS 2004. Figure 16 (first panel) is the same as figure 14 (first panel) but
393   presents the spatial distribution of the TXn index. CPC-T2m observation displays maxima
394   (greater than 36°C) and minima (less than 24°C) of TXn over the Sahara and the Guinea Coast
395   respectively (Fig.16a, c).
396   The control experiments (Fig.16b, d) show a good agreement with the CPC-T2m datasets in the
397   large scale patterns with PCC of approximately 0.99, however, the magnitude of the TXn index
398   over most of studied domain is overestimated. The strongest positive bias was observed over
399   West Sahel domain with MB about 6.56 and 5.44 °C for JJAS 2003 and JJAS 2004, respectively
400   (Table 4). The TXn biases of our study are lower than those obtained by Thanh et al. (2017) in
401   their work over Asia using RegCM4. As for Fig.14 (second panel), the Figure 16 (second panel)
402   displays changes in TXn index. Dry experiments increase TXn index values while the wet
403   experiments decrease them.

404

405   Figure 16 (second panel) is similar to figure 14 (second panel) but displays the PDF distribution
406   of changes in TXn. The impact on TXn is rather weak compared to the TXx. The strongest
407   increase of TXn index are found over the Central Sahel reaching 1.03 °C in dry experiments
408   during JJAS 2004 (Table 5). While the strongest decrease is found over the West Sahel about -
409   1.67°C for wet experiments during JJAS 2004 (Table 5).
410   In summary, RegCM4 overestimates the lowest day's temperature during JJAS 2003 and JJAS
411   2004 over the whole West African domain. As for TXx index, dry (wet) experiments increase
412   (decrease) the TXn values.

413

414   **3.2.3. Minimum value of daily minimum temperature (TNn index).**
415   In this section, we examined the TNn index, which gives the lowest temperature at night during
416   JJAS 2003 and JJAS 2004. Figure 18 (first panel) is the same as figure 14 (first panel) but
417   displays the spatial distribution of the TNn index. CPC-T2m observations (Fig. 18 a, c) shows

TNn maxima with values not exceeding 27 °C, above 15 °N latitude, while the minima values (less than 17 °C) are found over the mountainous regions such as the Cameroon Mountains, Jos Plateau, and Guinea Highlands.

The control experiments (Fig. 18 b, d) show good agreement with CPC-T2m observations with PCC of approximately 0.99; however, they exhibit some biases at the local scale. The control experiments overestimate the magnitude of the TNn index over most of studied domains. The strongest positive biases are found over the West Sahel with MB reaching 3.30 °C and 2.55 °C for JJAS 2003 and JJAS 2004, respectively (Table 4). These positive biases obtained for the TXx, TXn, and TNn indices are opposite to the cold bias known from RegCM4 in mean climate simulation (Koné et al., 2018, Klutse et al., 2016). It is difficult to determine the origin of RegCM4 temperature biases, as they can depend on several factors, such as surface energy fluxes and water, cloudiness, and surface albedo (Sylla et al., 2012; Tadross et al., 2006).

Figure 18 (second panel) is the same as figure 14 (second panel), but displays changes in the TNn. Over the Central and West Sahel, both dry and wet experiments decrease the TNn values. Conversely, over the Guinea Coast, they increase the TNn values.

Figure 19 is the same as Figure 15 but shows the PDF distribution of changes in the TNn. Wet (dry) experiments increase (decrease) the TNN values, especially over the Central Sahel. Table 5 shows that the strongest increase in TNn index in wet experiments is found over Guinea Coast, with maximum change around 0.11 °C in JJAS 2004, while the strongest decrease in TNn is found in dry experiments over the West Sahel, with maximum change around −1.15 °C in JJAS 2003.

In summary, RegCM4 overestimates the lowest temperature at night during JJAS 2003 and JJAS 2004. Wet (dry) experiments lead to an increase (a decrease) of the TNN index.

3.2.4. Maximum value of daily minimum temperature (TNx)

In this section, the index TNx which gives the warmest night temperature during JJAS 2003 and JJAS 2004 is analyzed. Figure 20 (first panel) is the same as figure 14 (first panel), but for the TNx index. CPC-T2m observation (Fig. 20a, c) shows the maxima of the TNx index over the Sahara with values reaching 40 °C, while the minima around 24 °C are located over the Guinea Coast.

The control experiments (Fig. 20b, d) well reproduced the general features of the TNx index with a PCC value reached 0.99, but some differences exist at local scale. Unlike the TNn index,

451   control experiments underestimate the TNx over most of the studied domain. The strongest

452   negative biases are found over the Central Sahel, with MB values up to -3.35 °C and -3.32 °C

453   for JJAS 2003 and JJAS 2004, respectively (Table 4). The TNx index underestimation seems

454   to be systematically related to the cold bias in RegCM4 over West Africa, which has been

455   reported in several papers (Koné et al., 2018, Klutse et al., 2016).

456   Figure 20 (second panel) is the same as figure 14 (second panel) but displays changes in the

457   TNx. Like for TNn index, over the Central Sahel, dry experiments increase the TNx values,

458   while the wet experiments decrease them. However, over the West Sahel, both wet and dry

459   experiments led to a dominant decrease. Conversely, over the Guinea Coast, although the signal

460   is weak, both dry and wet experiments led to a dominant increase.

461   Figure 21 is the same as figure 15 but displays the PDF distributions of the changes in the TNx.

462   The highest TNx increase (decrease) is found over the Central Sahel in dry (wet) experiments

463   with maximum changes up to 0.25 (-1.67 °C) for JJAS 2003 (JJAS 2004) (Table 5). In

464   summary, RegCM4 underestimates the warmest night temperature and dry (wet) experiments

465   lead to an increase (decrease) of TNx magnitude.

466

467   **4. Conclusions**

468   The impact of the soil moisture initial conditions on six precipitation extreme indices and four

469   temperature extreme indices over West Africa was investigated using the RegCM4-CLM45.

470   We first evaluated the performance of RegCM4-CLM4.5 in representing these climate extreme

471   indices over West Africa. We then performed sensitivity studies over the West African domain,

472   with a spatial resolution of 25 km. We initialized the control runs using ERA20C reanalysis soil

473   moisture and for dry and wet experiments, we used the maximum and minimum values of

474   ERA20C over the whole domain, respectively. Results have been presented for JJAS 2003 and

475   JJAS 2004 which are the two contrasted runs most sensitive to the effects of dry and wet soil

476   moisture initial conditions.

477   Compared to CHIRPS observation, the model overestimates and underestimates the number of

478   wet days. RegCM4 also underestimates the simple daily precipitation intensity index (SDII),

479   the maximum 1-day precipitation (Rx1day), and the precipitation percentage due to very heavy

480   precipitation days (R95pTOT). The current physical parameterization scheme of the RegCM4

481   model used in our study results in a positive bias of the number of wet days with a low

482   precipitation threshold (e. g. 1 mm.day^{-1}), and in a negative bias for a higher precipitation

483   threshold (e.g. 10 mm.day^{-1}, not shown here). RegCM4 generally overestimates the CWD and

484   CDD indices over West Africa. Most of the temperature extreme indices used in this study

485   (TXx, TXn, and TNn) are also overestimated, except the TNx index, which is underestimated

486   over the West Africa domain.

487   The impact on extreme precipitation indices of the soil moisture initial conditions is linear over

488   the Sahel central, only for indices related to the number of precipitation events (R1mm, CDD,

489   and CWD indices) meaning that wet (dry) experiments lead to an increase (decrease) of the

490   number of days, and not for those related to the amount or intensity of precipitation (SDII,

491   RX1day, and R95pTOT). However, the dry and wet experiments increase the precipitation

492   percentage due to very heavy precipitation days and the maximum one-day precipitation

493   accumulation (R95pTOT and RX1day indices, respectively) over most of the studied domain.

494   The soil moisture initial conditions unequally influence the daily maximum and minimum

495   temperatures over the West African domain. The impact on daily maximum temperature

496   extremes are greater than those on the daily minimum temperature extremes. These results are

497   consistent with previous studies (Jaeger and Seneviratne, 2011; Zhang et al., 2009).The wet

498   (dry) experiments lead to TXx and TXn increase (decrease) over West Africa. However,

499   regarding the minimum temperature we showed that dry (wet) experiments lead to a TNx

500   increase (decrease).

501   This study helped to quantify the impact of the soil moisture initial conditions on precipitation

502   and temperature extreme events in terms of intensity, frequency and duration over West Africa.

503   This study is the first to investigate the impact of soil moisture initial conditions on climate

504   extreme indices over West Africa. These experiments were done in a highly-idealized framework

505   and were intended to show the potential impact of very strong soil moisture initial conditions on

506   climate extremes. Consequently, it should be considered as a first overview of the influence of

507   initial soil moisture on climate extremes with a RCM (RegCM4). This study will benefit from

508   being performed in a multi-model framework with several RCMs within CORDEX-Africa

509   initiative (Coordinated Regional Downscaling Experiment).

510   **Author contribution**

511   The authors declare to have no conflict of interest with this work. B. Koné and A. Diedhiou

512   fixed the analysis framework. B. Koné carried out all the simulations and figures production

513 according to the outline proposed by A. Diedhiou. B. Koné and A. Diedhiou, S. Anquetin and

514 A. Diawara worked on the analyses. All authors contributed to the drafting of this manuscript.

515

516 **Acknowledgements**

517 The research leading to this publication is co-funded by the NERC/DFID "Future Climate for

518 Africa" programme under the AMMA-2050 project, grant number NE/M019969/1 and by

519 IRD (Institut de Recherche pour le Développement; France) grant number UMR IGE

520 Imputation 252RA5.

521

522 **References:**

523

524 Bichet, A., & Diedhiou, A. : West African Sahel has become wetter during the last 30 years,

525 but dry spells are shorter and more frequent. Climate Research, 75(2), 155-162, (2018a)

526

527 Bichet, A., & Diedhiou, A.: Less frequent and more intense rainfall along the coast of the Gulf

528 of Guinea in West and Central Africa (1981 2014). Climate Research, 76(3), 191-201, (2018b)

529

530 Damien Decremer, Chul E. Chung, Annica M. L. Ekman & Jenny Brandefelt (2014) Which

531 significance test performs the best in climate simulations?, Tellus A: Dynamic Meteorology

532 and Oceanography, 66:1, DOI: 10.3402/tellusa.v66.23139.

533

534 Danielson J.J., and Gesch D.B.: Global multi-resolution terrain elevation data 2010

535 (GMTED2010): U.S. Geological Survey Open-File Report 2011–1073, 26 p, 2011.

536

537 Didi Sacré Regis M , Mouhamed, L., Kouakou, K., Adeline, B., Arona, D., Koffi Claude A, K.,

538 ... & Issiaka, S. (2020). Using the CHIRPS Dataset to Investigate Historical Changes in

539 Precipitation Extremes in West Africa. Climate, 8(7), 84.

540

541 Diaconescu E. P., Gachon P. , Scinocca J., and LapriseR.: Evaluation of daily precipitation

542 statistics and monsoon onset/retreat over West Sahel in multiple data sets. Climate Dyn., 45,

543 1325–1354, doi:10.1007/s00382-014-2383-2, 2015 .

544

545 Easterling, D.R., Meehl, G.A., Parmesan, C., Changnon, S.A., Karl, T.R. and Mearns, L.O.:

546 Climate Extremes: Observations, Modeling and Impacts. Science , 289, 2068-2074.

547 https://doi.org/10.1126/science.289.5487.2068, 2000.

548

549 Emanuel K. A.: A scheme for representing cumulus convection in large-scale models. Journal

550 of the Atmospheric Science 48: 2313–2335, 1991.

551

552 Fan Y., and van den Dool H. : A global monthly land surface air temperature analysis for 1948

553 -present, J. Geophys. Res. 113, D01103, doi: 10.1029/2007JD008470, 2008.

554

555 Folland C. K., Palmer T. N. , and Parker D. E.: Sahel rainfall and worldwide sea

556 temperatures, Nature, 320, 602 – 607, 1986.

557

558 Fontaine B., Janicot S. , and Moron V. : Rainfall anomaly patterns and wind field signals over

559 West Africa in August (1958 – 1989), J. Clim., 8, 1503 –1510, 1995.

560

561 Giorgi F., Coppola E., Solmon F., Mariotti L., Sylla M. B., Bi X., Elguindi N., Diro G. T., Nair

562 V., Giuliani G., Cozzini S., Guettler I., O'Brien T., Tawfik A., Shalaby A., Zakey A. S., Steiner

563 A., Stordal F., Sloan L., and Brankovic C. : RegCM4: model description and preliminary tests

564 over multiple CORDEX domains, Clim. Res., 52, 7–29, doi.org/10.3354/cr01018, 2012.

565

566 Grell G., Dudhia J. and Stauffer D. R.: A description of the fifth generation Penn State/NCAR

567 Mesoscale Model (MM5), National Center for Atmospheric Research Tech Note NCAR/TN-

568 398+STR, NCAR, Boulder, CO, 1994.

569

570 Holtslag A., De Bruijn E., and Pan H. L. : A high resolution air mass transformation model for

571 short-range weather forecasting, Mon. Weather Rev., 118, 1561–1575, 1990.

572

573 Hong S. Y. and Pan H. L.: Impact of soil moisture anomalies on seasonal, summertime

574 circulation over North America in a regional climate model. J. Geophys. Res., 105 (D24), 29

575 625–29 634, 2000.

576

577 Jaeger E. B., and Seneviratne S. I. : Impact of soil moisture-atmosphere coupling on

578 European climate extremes and trends in a regional climate model, Clim. Dyn., 36(9-10),

579 1919-1939, doi:10.1007/s00382-010-0780-8, 2011.

580

581 Kang S, Im E.-S. and Ahn J.-B.: The impact of two land-surface schemes on the characteristics

582 of summer precipitation over East Asia from the RegCM4 simulations Int. J. Climatol. 34:

583 3986–3997, 2014.

584

585 Kim J-E., and Hong S-Y.: Impact of Soil Moisture Anomalies on Summer Rainfall over East

586 Asia: A Regional Climate Model Study, Journal of Climate. Vol. 20, 5732–5743, DOI:

587 10.1175/2006JCLI1358.1, 2006.

588

589 Kiehl J. T., Hack J. J., Bonan G. B., Boville, B. A., Briegleb B. P., Williamson D. L., and Rasch

590 P. J.: Description of the NCAR Community Climate Model (CCM3), Technical Note

591 NCAR/TN−420+STR, 152, 1996.

592

593 Koné B., Diedhiou A., N'datchoh E. T., Sylla M. B. , Giorgi F., Anquetin S., Bamba A.,

594 Diawara A., and Kobea A. T.: Sensitivity study of the regional climate model RegCM4 to

595 different convective schemes over West Africa. Earth Syst. Dynam., 9, 1261–1278.

596 https://doi.org/10.5194/esd-9-1261-2018, 2018.

597

598

599 Koster R. D., GUO Z. H., Dirmeyer P. A., Bonan G., Chan E., Cox P., Davies H., Gordon C.

600 T., Gordon C. T.,Lawrence D., Liu P., Lu C. H, Malyshev S., McAvaney B., Mitchell K, Mocko

601 D., Oki K., Oleson K., Pitman A., Sud Y. C. , Taylor C. M., 16 Verseghy D., Vasic R., Xue

602 Y.,   Yamada T.: The global land–atmosphere coupling experiment. Part I: Overview, J.

603 Hydrometeorol., 7(4), 590–610, doi:10.1175/JHM510.1, 2006.

604

605 Larsen J.: Record heat wave in Europe takes 35,000 lives. Earth Policy Institute, 2003.

606

607 Le Barbé L., Lebel L., and Tapsoba D.: Rainfall variability in west africa during the years 1950-
608 1990. J. Climate, 15 :187–202., 2002.

609

610 Loveland TR, Reed BC, Brown JF, Ohlen DO, Zhu Z, Yang L, J. W. Merchant J. W.:
611 Development of a global land cover characteristics database and IGBP DISCover from 1km
612 AVHRR data. International Journal of Remote Sensing 21: 1303–1330, 2000.

613

614 Liu D., G. Wang R. Mei Z. Yu, and Yu M. : Impact of initial soil moisture anomalies on climate
615 mean and extremes over Asia, J. Geophys. Res. Atmos., 119, 529–545,
616 doi:10.1002/2013JD020890, 2014.

617

618 Klutse B. A. N., Sylla B. M., Diallo I., Sarr A., Dosio A.,Diedhiou A., Kamga A., Lamptey B.,
619 Ali A., Gbobaniyi E. O., Owusu K., Lennard C., Hewitson B., Nikulin G.,& Panitz H.-J.,
620 Büchner M.: Daily characteristics of West African summer monsoon precipitation in CORDEX
621 simulations. Theor Appl Climatol. 123:369–386 DOI 10.1007/s00704-014-1352-3, 2016.

622

623 Menéndez, C. G., Giles, J., Ruscica, R., Zaninelli, P., Coronato, T., Falco, M., ... & Li, L.
624 (2019). Temperature variability and soil–atmosphere interaction in South America simulated
625 by two regional climate models. Climate Dynamics, 53(5), 2919-2930.

626

627 Nicholson, SE.: The nature of rainfall fluctuations in subtropical West-Africa. Mon. Wea. Rev.
628 22109, 2191-2208, 1980.

629

630 Nicholson SE.: Land Surface processes and Sahel climate. Reviews of Geophysics. 38(1), 117-
631 24139, 2000.

632

633 Nikulin G., Jones C., Samuelsson P., Giorgi F., Asrar G., Büchner M., Cerezo-Mota R.,
634 Christensen O. B., Déque M., Fernandez J., Hansler A., van Meijgaard E., Sylla M. B. and
635 Sushama L.: Precipitation climatology in an ensemble of CORDEX-Africa regional climate
636 simulations, J. Climate, 6057–6078, https://doi.org/10.1175/JCLI-D-11-00375.1, 2012.

637

638   Oleson K., Lawrence D. M., Bonan G. B., Drewniak B., Huang M., Koven C. D., Yang Z.-L.:

639   Technical description of version 4.5 of the Community Land Model (CLM) (No. NCAR/TN-

640   503+STR). doi:10.5065/D6RR1W7M, 2013.

641

642   Pal J. S., Small E. E. and Elthair E. A.: Simulation of regional scale water and energy budgets:

643   representation of subgrid cloud and precipitation processes within RegCM, J. Geophys. Res.,

644   105, 29579–29594, 2000.

645

646   Pan, Y.; Wang, W.; Shi, W. Assessment of CPC-T2m Global Daily Surface Air Temperature

647   (CPC-T2m) Analysis. Assessment 2019, 22, 24.

648

649   Peterson T. C., Folland C., Gruza G., Hogg W. Mokssit A., Plummer N. : Report on the

650   activities of the working group on climate change detection and related rapporteurs 1998-2001.

651   Geneva (Switzerland): WMO Rep. WCDMP 47, WMO-TD 1071, 2001.

652

653   Philippon N., Mougin E. , Jarlan L. , and Frison P.-L.: Analysis of the linkages between

654   rainfall and land surface conditions in the West African monsoon through CMAP, ERS-

655   WSC,and NOAA-AVHR R data. J. Geophys. Res., 110, D24115,

656   doi:10.1029/2005JD006394, 2005.

657

658   Reynolds, R. W. and Smith, T. M.: Improved global sea surface temperature analysis using

659   optimum interpolation, J. Climate, 7, 929–948, 1994.

660

661   Simmons A. S., Uppala D. D. and Kobayashi S.: ERA-interim: new ECMWF reanalysis

662   products from 1989 onwards, ECMWF Newsl., 110, 29–35, 2007.

663   Solmon F., Giorgi F., and Liousse C.: Aerosol modeling for regional climate studies:

664   application to anthropogenic particles and evaluation over a European/African domain, Tellus

665   B, 58, 51–72, 2006.

666

667   Sundqvist H. E., Berge E., and Kristjansson J. E.: The effects of domain choice on summer

668   precipitation simulation and sensitivity in a regional climate model, J. Climate, 11, 2698–2712,

669   1989.

670

671   Sylla MB, Giorgi F, Stordal F.: Large-scale origins of rainfall and temperature bias in high

672   resolution simulations over Southern Africa. Climate Res. 52: 193–211, DOI: 10.3354/cr01044,

673   2012.

674

675   Tadross MA, Gutowski WJ Jr, Hewitson BC, Jack C, New M.: MM5 simulations of interannual

676   change and the diurnal cycle of southern African regional climate. Theor. Appl. Climatol. 86(1–

677   4):63–80, 2006.

678

679   Takahashi, H. G., & Polcher, J. (2019). Weakening of rainfall intensity on wet soils over the

680   wet Asian monsoon region using a high-resolution regional climate model. Progress in Earth

681   and Planetary Science, 6(1), 1-18.

682

683   Thanh N.-D., Fredolin T. T., Jerasorn S., Faye C., Long T.-T., Thanh N.-X., Tan P.-V., Liew

684   J., Gemma N., Patama S., Dodo G. and Edvin A.: Performance evaluation of RegCM4 in

685   simulating extreme rainfall and temperature indices over the CORDEX-Southeast Asia region.

686   Int. J. Climatol. 37: 1634–1647. Published online 28 June 2016 in Wiley Online Library

687   (wileyonlinelibrary.com) DOI: 10.1002/joc.4803, 2017.

688

689   Uppala S., Dee D., Kobayashi S., Berrisford P. and Simmons A.: Towards a climate data

690   assimilation system: status update of ERA-interim, ECMWF Newsl., 15, 12–18, 2008.

691

692   Wang, G., Yu, M., Pal, J. S., Mei, R., Bonan, G. B., Levis, S., and Thornton, P. E.: On the

693   development of a coupled regional climate vegetation model RCM-CLM-CN-DV and its

694   validation its tropical Africa, Clim. Dynam, 46, 515–539, 2016.

695

696   You Q., Kang S., Aguilar E., Pepin N., Flügel W.-A., Yan Y. , Xu Y., Zhang Y. , and Huang

697   J. : Changes in daily climate extremes in China and their connection to the large scale

698   atmospheric circulation during 1961–2003, Clim. Dyn., 36(11-12), 2399–2417,

699   doi:10.1007/s00382-009-0735-0, 2010.

700

701   Zakey A. S., Solmon F., and Giorgi F.: Implementation and testing of a desert dust module in

702   a regional climate model, Atmos. Chem. Phys., 6, 4687–4704, https://doi.org/10.5194/acp-6-

703   4687-2006, 2006.

704

705   Zeng X., Zhao M. and Dickinson R .E.: Intercomparison of bulk aerodynamic algorithms for

706   the computation of sea surface fluxes using TOGA COARE and TAO DATA, J. Climate, 11,

707   2628-2644, 1998.

708

709   Zhang J, Wang W.C., and Wu L.: Land–atmosphere coupling and diurnal temperature range

710   over the contiguous United States. Geophys Res Lett 36:L06706. doi:10.1029/2009GL037505,

711   2009.

712

713   Zhang J. Y., Wu L. Y. and Dong W.: Land-atmosphere coupling and summer climate

714   variability over East Asia, J. Geophys. Res., 116,D05117, doi 10.1029/2010JD014714, 2011.

715

716

717

718

719

720

721

722

723

724

725

726

727

728

729

730

731

732

 TABLES AND FIGURES.

	Extreme indices	Definition	Units
Extreme Rainfall Indices			
1	R1mm	Number of wet days (daily precipitation $\geq$ 1mm)	day
2	SDII	The amount of precipitation mean on wet days (daily precipitation $\geq$ 1mm)	$mm.day^{-1}$
3	CDD	Maximum number of consecutive dry days (daily precipitation $<$ 1 $mm.day^{-1}$)	day
4	CWD	Maximum number of consecutive wet days (daily precipitation $\geq$ 1 $mm.day^{-1}$)	day
5	RX1day	The maximum one-day precipitation accumulation	mm
6	R95pTOT	Precipitation percent due to very heavy precipitation days.	%
Extreme temperature indices			
7	TXn	Minimum value of daily maximum temperature	°C
8	TXx	Maximum value of daily maximum temperature	°C
9	TNn	Minimum value of daily minimum temperature	°C
10	TNx	Maximum value of daily minimum temperature	°C

735

736 **Table1**: The 10 extreme climate indices used in this study.

737

738

739

740

741

		Central Sahel		West Sahel		Guinea Coast		West Africa	
		MB	PCC	MB	PCC	MB	PCC	MB	PCC
R1mm	CTRL_2003	33.17	0.98	-5.25	0.96	**53.16**	0.96	22.18	**0.96**
	CTRL_2004	29.50	0.98	1.34	0.96	**55.46**	0.96	23.85	**0.95**
SDII	CTRL_2003	-7.52	0.97	-9.95	0.94	**-13.62**	0.77	-7.67	**0.73**
	CTRL_2004	-7.01	0.97	-9.37	0.94	**-14.65**	0.81	-7.59	**0.77**
CDD	CTRL_2003	0.93	0.90	**14.49**	0.91	**-7.84**	0.66	**2.63**	**0.85**
	CTRL_2004	4.75	0.91	**17.51**	0.95	**-9.43**	0.68	**6.99**	**0.89**
CWD	CTRL_2003	45.56	0.83	18.44	0.75	**59.21**	0.88	31.20	**0.81**
	CTRL_2004	36.78	0.79	20.48	0.78	**60.51**	0.82	29.74	**0.79**
RX1day	CTRL_2003	-26.46	0.78	**-38.07**	0.91	**-30.28**	0.54	-20.08	**0.50**
	CTRL_2004	-22.89	0.46	**-36.67**	0.88	**-42.44**	0.42	-20.23	**0.40**
R95pTOT	CTRL_2003	-27.67	0.67	-33.39	0.77	**-43.22**	0.65	-29.12	**0.59**
	CTRL_2004	-24.38	0.46	-31.75	0.80	**-46.61**	0.60	-27.45	**0.55**

742

Table 2: The pattern correlation coefficient (PCC) and the mean bias (MB) of R1mm (in day), SDII (in mm.day-1), CDD (in day), CWD (in day), RX1day (in mm) and R95pTOT (in %) indices for control experiments (initialized with initial soil moisture of ERA20C reanalysis) with respect to CHIRPS, calculated over Guinea Coast, Central Sahel, West Sahel and the entire West African domain for JJAS 2003 and JJAS 2004.

748

749

750

751

752

Precipitation indices		Central Sahel		West Sahel		Guinea Coast		West Africa	
		ΔWC	ΔDC	ΔWC	ΔDC	ΔWC	ΔDC	ΔWC	ΔDC
R1mm (day)	2003	8.14	**-5.19**	**12.02**	0.69	3.92	2.88	4.67	1.75
	2004	10.01	-3.79	10.14	0.56	4.90	3.57	7.90	2.61
SDII (mm/day)	2003	0.07	0.11	-0.11	0.14	0.70	0.17	0.29	0.31
	2004	0.03	0.09	0.26	-0.07	0.56	0.22	0.24	0.21
CWD (day)	2003	13.25	-3.15	6.61	0.64	12.24	4.05	9.43	1.09
	2004	**15.58**	**-4.48**	7.20	-0.19	6.08	3.18	11.89	-0.37
CDD (day)	2003	-2.80	2.58	**-12.73**	0.83	-0.68	-1.31	-1.53	0.19
	2004	-5.92	**3.80**	-7.75	2.75	-0.93	-1.46	-3.57	-0.44
RX1day (mm)	2003	1.97	3.78	0.11	0.65	**26.14**	4.17	7.16	7.27
	2004	3.35	3.03	7.05	0.19	**14.93**	15.73	6.46	2.28
R95pTOT (%)	2003	1.54	1.77	2.88	1.53	**4.33**	2.37	2.83	2.46
	2004	1.66	0.89	**4.03**	0.43	1.69	0.92	1.37	2.43

Table 3: Summary Table of maximum values of change on PDF's for R1mm, SDII, CDD, CWD, RX-1day and R95pTOT indices.

		Central Sahel		West Sahel		guinea		West Africa	
		MB	PCC	MB	PCC	MB	PCC	MB	PCC
TXx	CTRL_2003	2.10	0.99	**3.02**	0.99	-1.34	0.99	0.32	**0.99**
	CTRL_2004	1.14	0.99	**2.02**	0.99	-1.41	0.99	-0.16	**0.99**
TXn	CTRL_2003	5.12	0.99	**6.56**	0.99	3.76	0.99	**5.65**	**0.99**
	CTRL_2004	3.43	0.99	**5.44**	0.99	2.75	0.99	**4.14**	**0.99**
TNn	CTRL_2003	2.37	0.99	**3.30**	0.99	1.53	0.99	1.45	**0.99**
	CTRL_2004	2.09	0.99	**2.55**	0.99	1.28	0.99	0.71	**0.99**
TNx	CTRL_2003	-1.91	0.99	-2.86	0.99	**-3.35**	0.99	-3.85	**0.99**
	CTRL_2004	-1.90	0.99	-2.54	0.99	**-3.32**	0.99	-3.99	**0.99**

769

Table 4: The pattern correlation coefficient (PCC) and the mean bias (MB in°C) of TXx, TXn, TNn and TNx indices for control experiments (initialized with initial soil moisture of ERA20C reanalysis) with respect to CPC-T2m, calculated for Guinea Coast, Central Sahel, West Sahel and the entire West African domain for JJAS 2003 and JJAS 2004.

774

775

776

777

778

779

780

781

782

Temperature indices		Central Sahel		West Sahel		Guinea Coast		West Africa	
		ΔWC	ΔDC	ΔWC	ΔDC	ΔWC	ΔDC	ΔWC	ΔDC
TXx	2003	-2.54	1.14	-2.11	0.90	-0.34	0.68	-0.89	1.06
	2004	**-2.57**	**1.69**	-1.58	0.98	-0.32	1.01	-0.86	1.27
TXn	2003	-1.37	0.81	**-1.67**	-0.05	-0.06	0.28	-0.50	0.59
	2004	-1.09	**1.03**	-0.93	0.55	-0.04	0.31	-0.38	0.61
TNn	2003	-0.37	-0.20	-0.23	**-1.15**	0.05	0.04	-0.20	0.03
	2004	-0.03	-0.37	0.06	-1.07	**0.11**	-0.03	-0.05	-0.11
TNx	2003	-1.29	**0.25**	-0.94	-1.37	0.12	0.04	-0.49	0.13
	2004	**-1.67**	0.15	-0.62	-1.13	0.02	0.03	-0.51	-0.07

783

784 **Table 5:** Summary Table of maximum values of change on PDF's for TXx, TXn, TNn and
785 TNx indices.

786

787

788

789

790

791

792

793

794

795

796

797

798

799

800
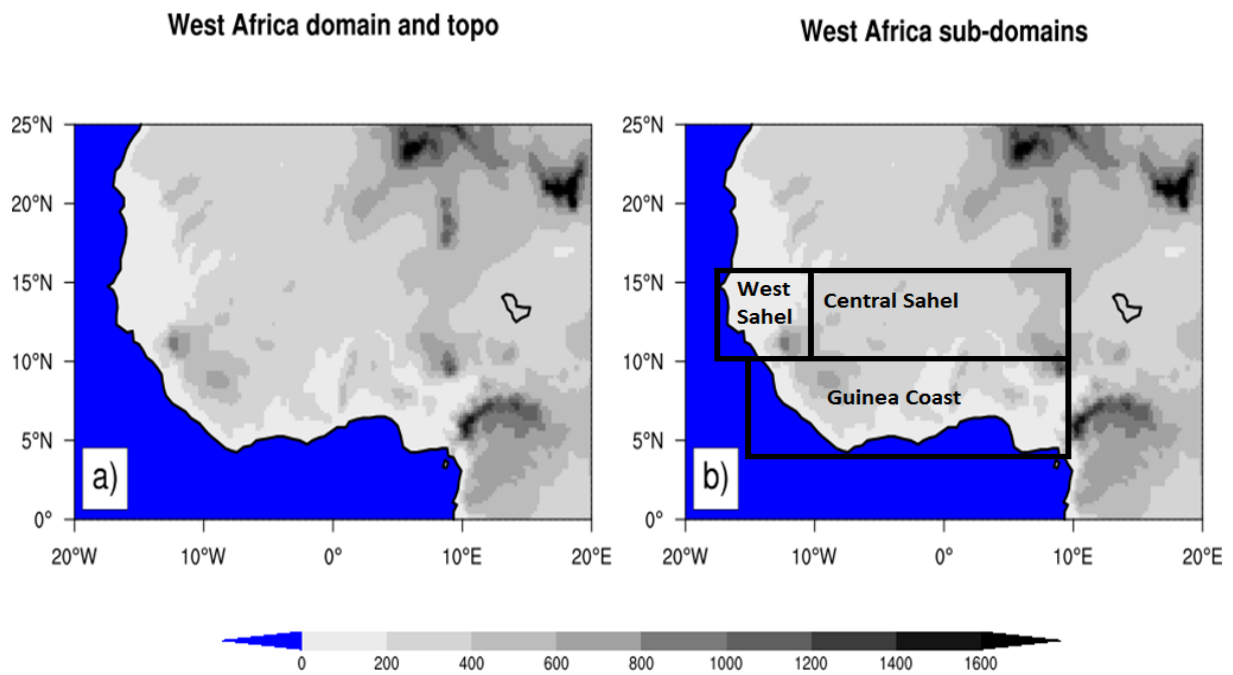
Figure 1: Topography of the West African domain. The analysis of the model result has an emphasis on the whole West African domain and the three subregions Guinea Coast, Central Sahel and West Sahel, which are marked with black boxes.
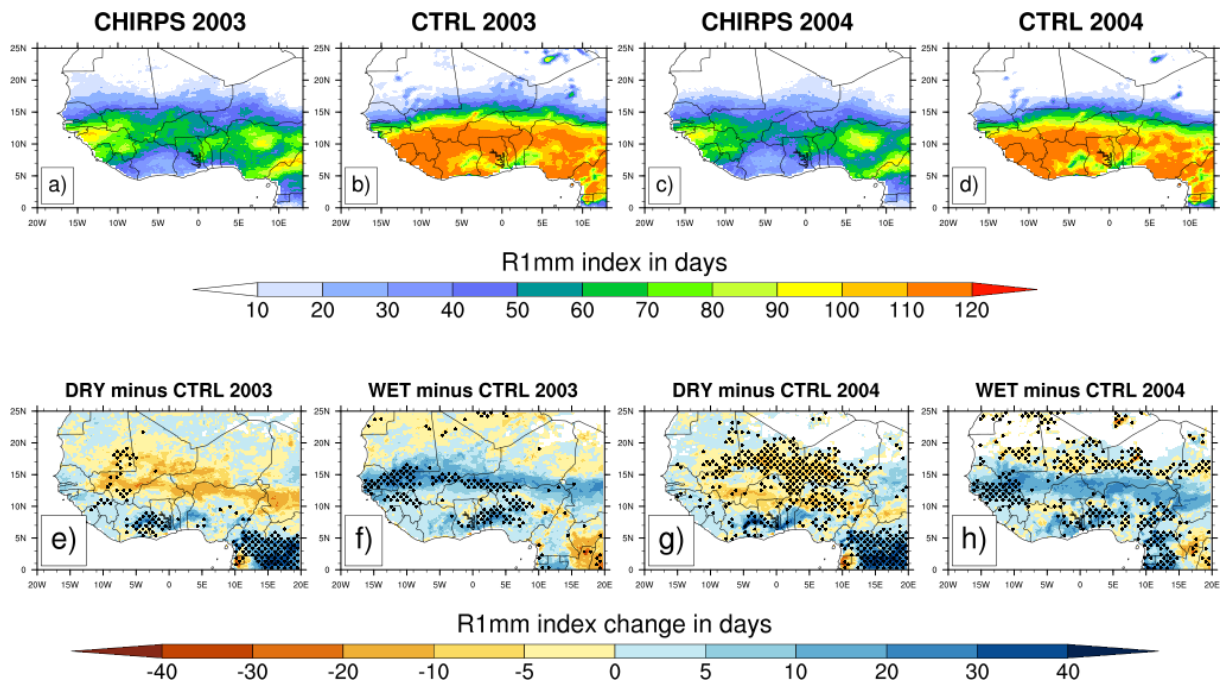
Figure2: Mean values of the number of the wet days (R1mm index in days) from CHIRPS (a and c) observation for JJAS 2003 and JJAS 2004 and the simulated control (CTRL) experiments (b and d) initialized with initial soil moisture of the reanalysis of ERA20C (first panel) and changes in R1mm index in days (second panel) for JJAS 2003 and JJAS 2004, from dry (e and g) and wet (f and h) experiments with respect to the control experiments. Areas with values passing the 95% significance test are dotted.
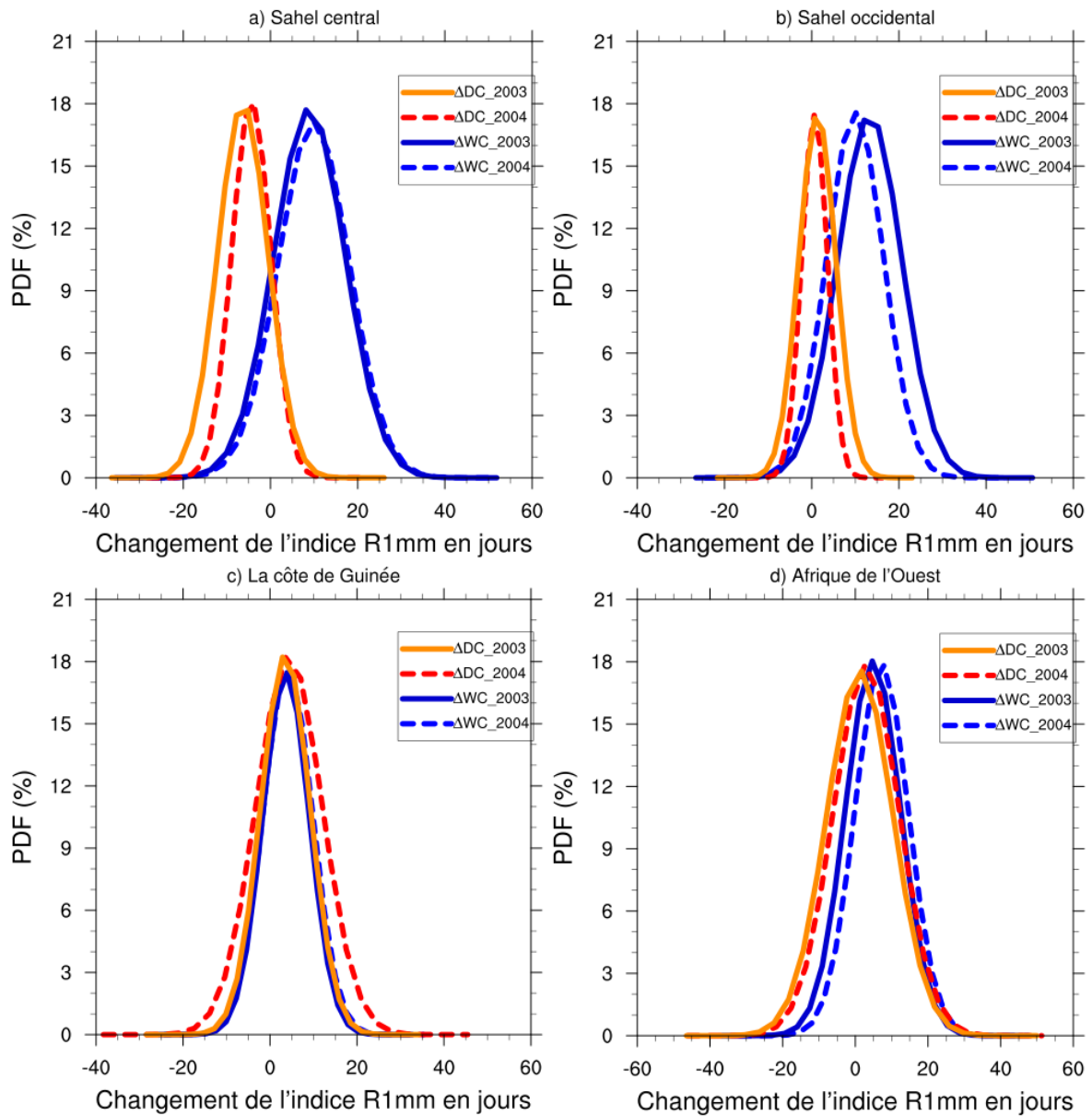
843

844 **Figure3:** PDF distributions (%) of mean values of the number of the wet days change in JJAS

845 2003 and JJAS 2004, over (a) Central Sahel, (b) West Sahel, (c) Guinea and (d) West Africa

846 derived from dry (ΔDC) and wet (ΔWC) experiments with respect to the control experiment.

847

848

849
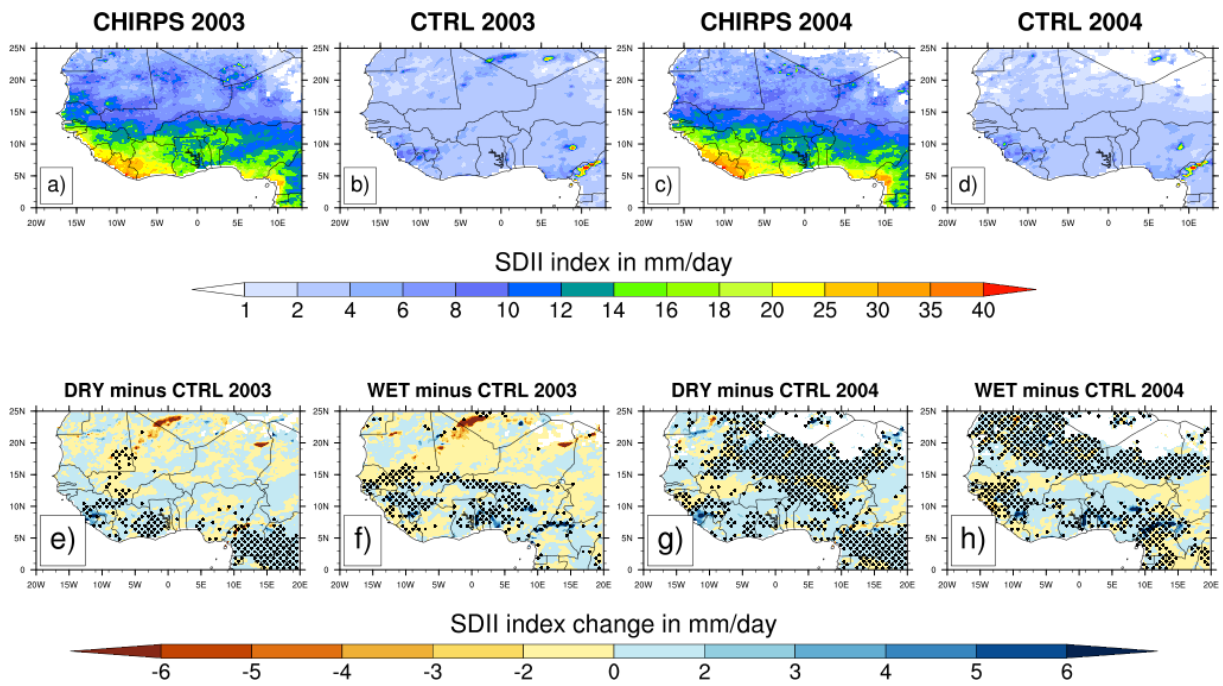
851

852 **Figure4:** Same as Fig. 2 but for the SDII index (in mm.day^{-1}).

853

854

855

856

857

858

859

860

861

862

863

864

865

866

867

868

869
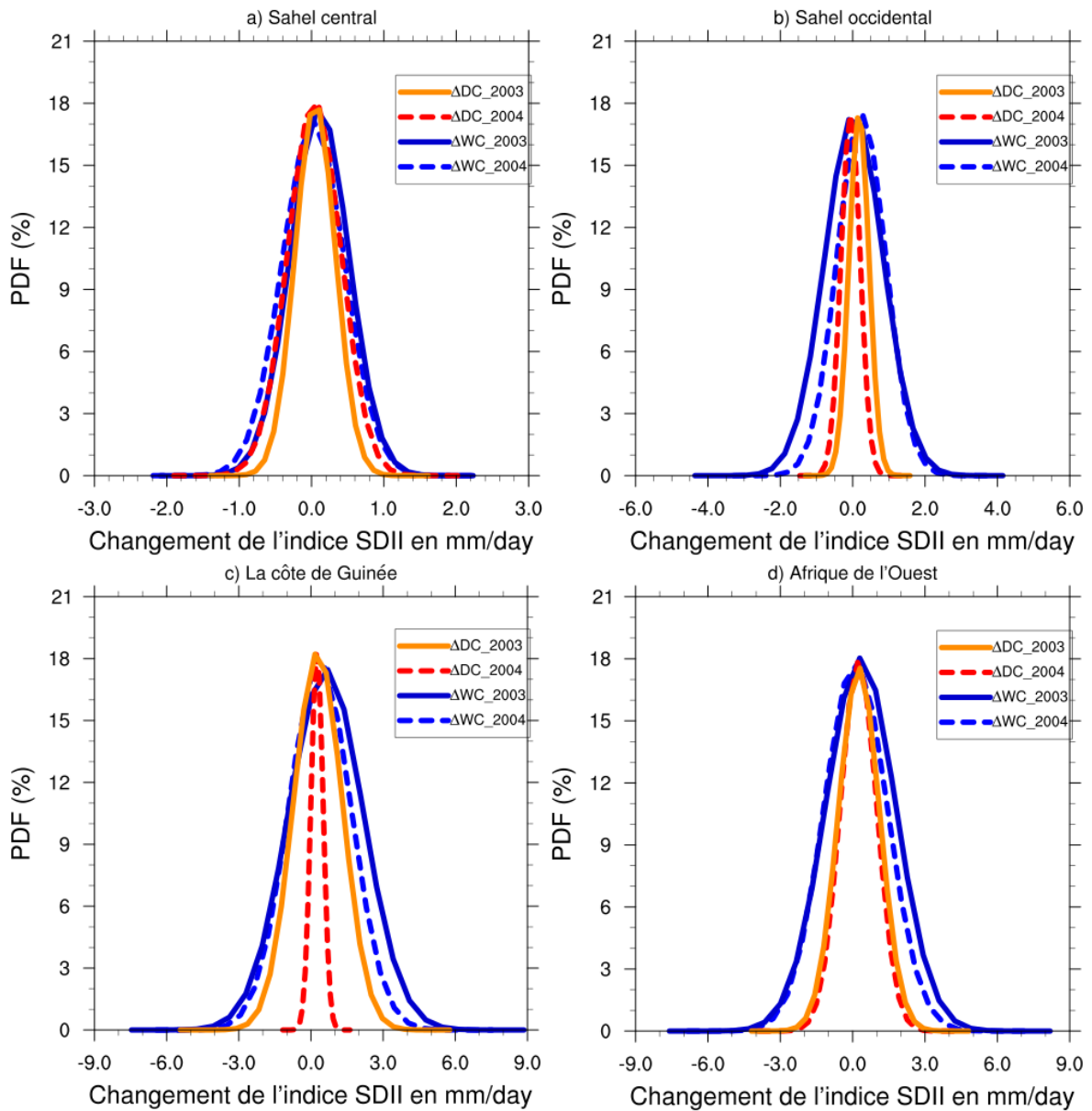
870 **Figure 5:** Same as Fig. 3 but for the SDII index (in mm.day^{-1}).

871

872

873

874

875

876
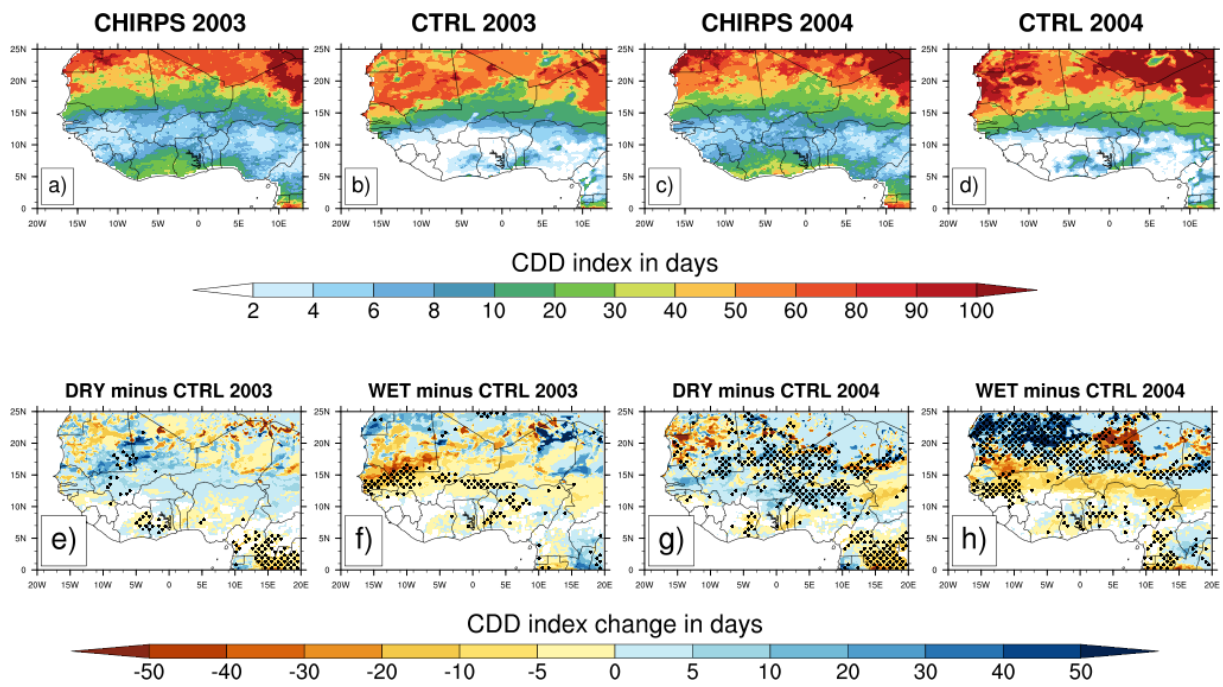
879

880 **Figure 6**: Same as Fig. 2 but for the CDD index (in day).

881

882

883

884

885

886

887

888

889

890

891

892

893

894
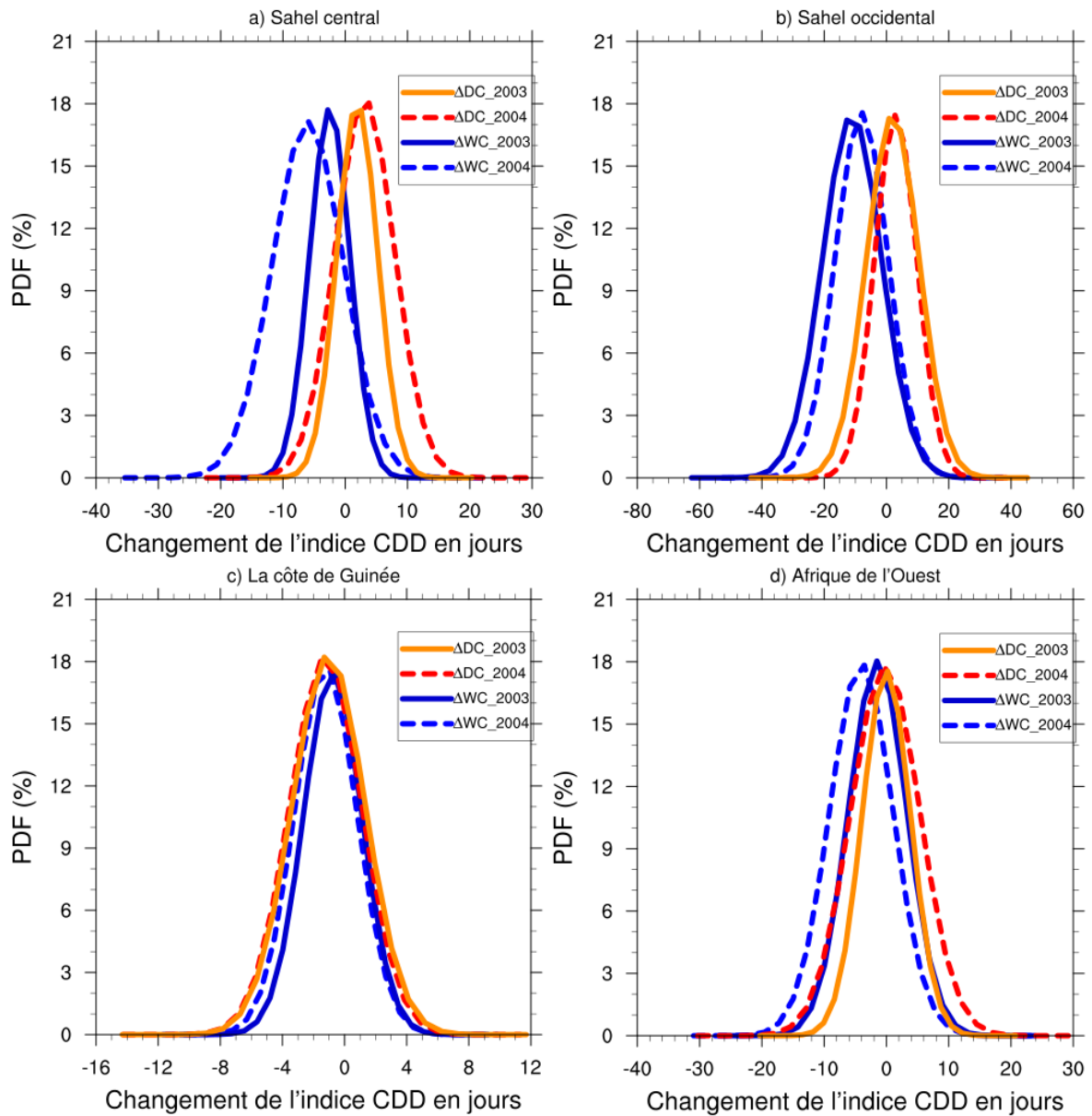
896
897
898 **Figure 7:** Same as Fig. 3 but for the CDD index (in day).

899
900
901
902
903
904
905
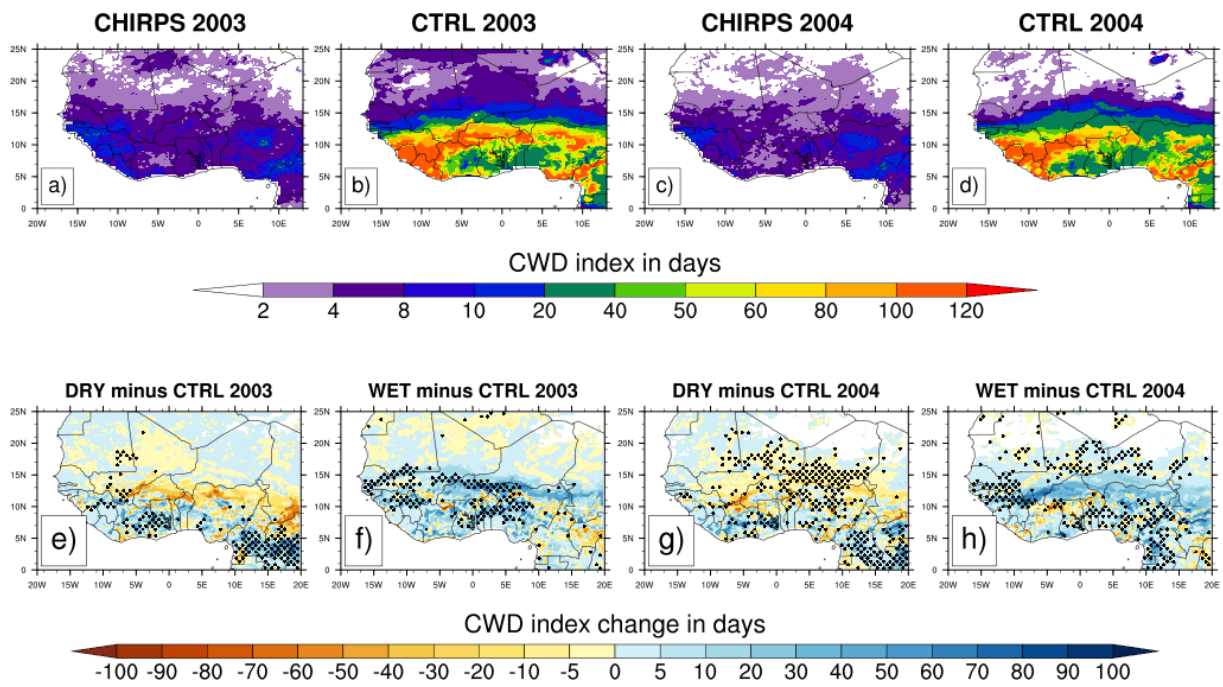
908

909 **Figure 8:** Same as Fig. 2 but for the CWD index (in day).

910

911

912

913

914

915

916

917

918

919

920

921

922

923

924

925
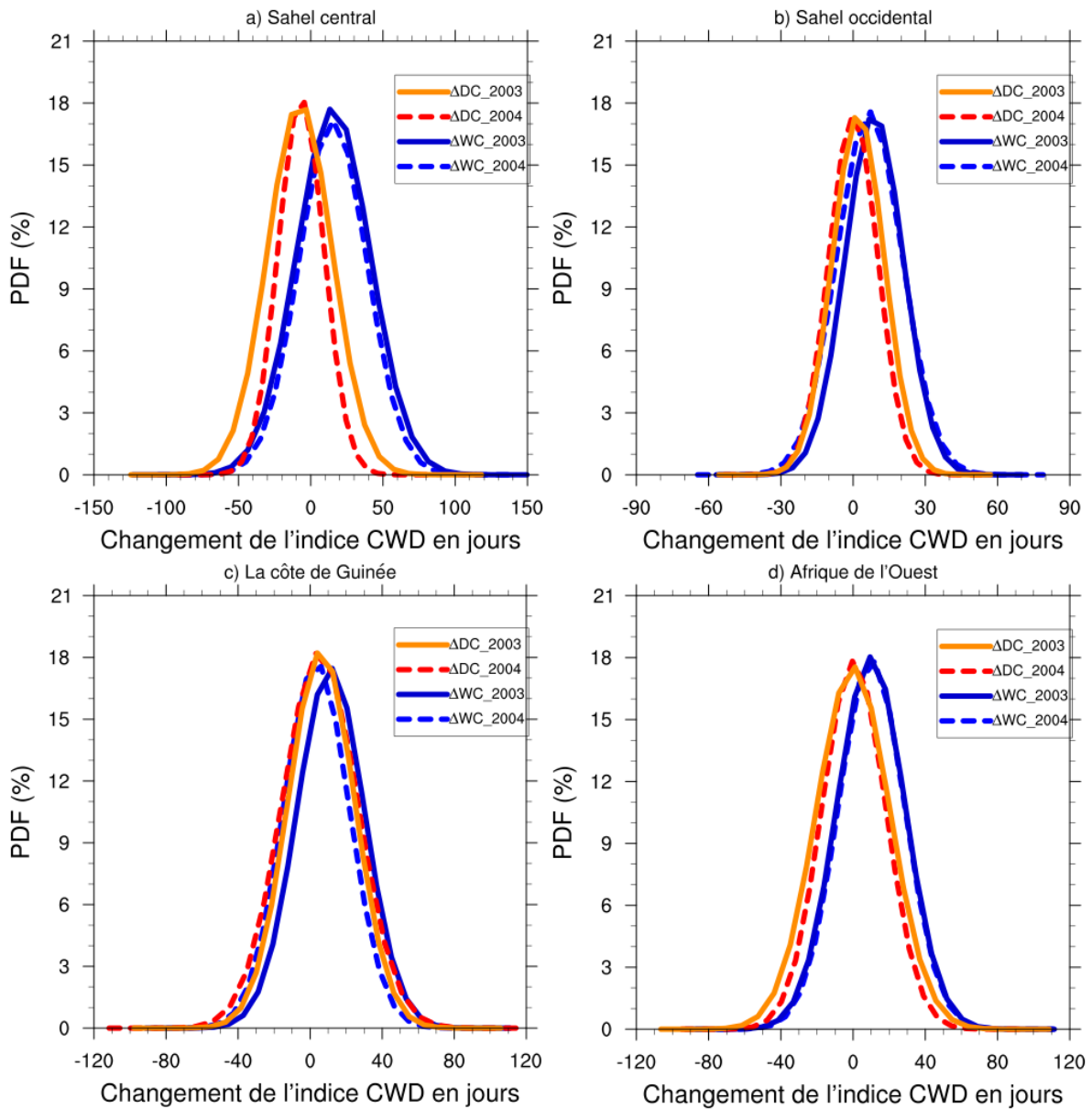
Figure 9: Same as Fig. 3 but for the CWD index (in day).
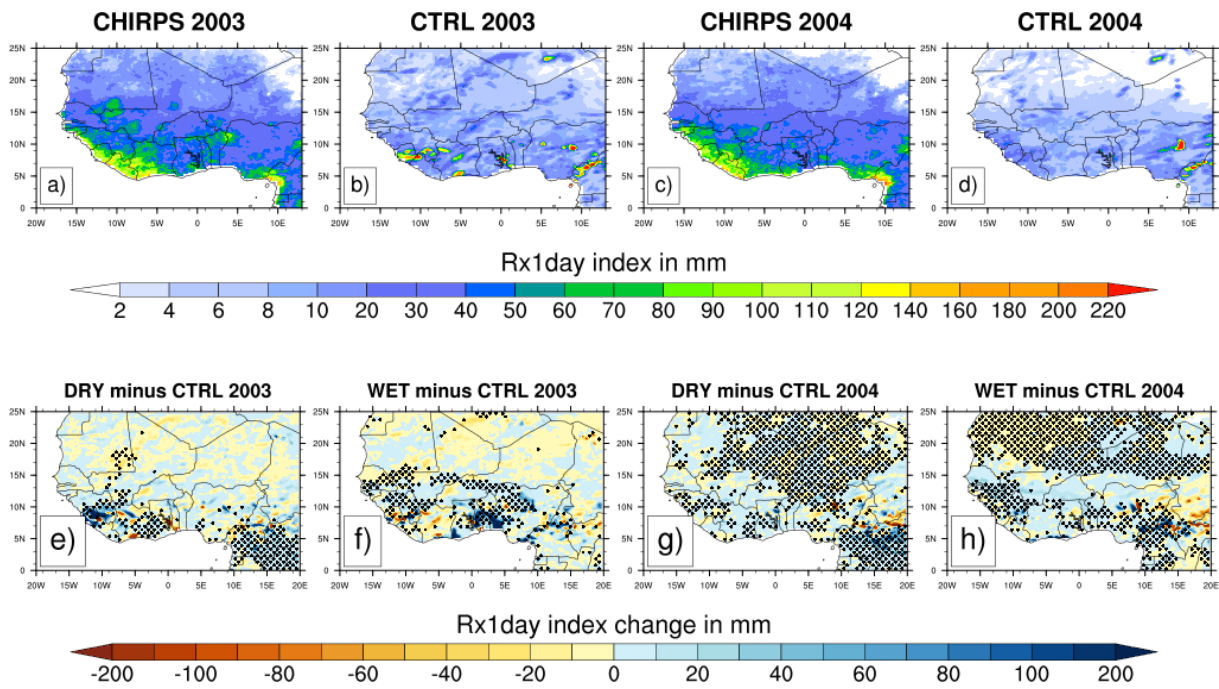
939

940 **Figure 10**: Same as Fig. 2 but for the RX1day index (in mm).

941

942

943

944

945

946

947

948

949

950

951

952

953

954

955
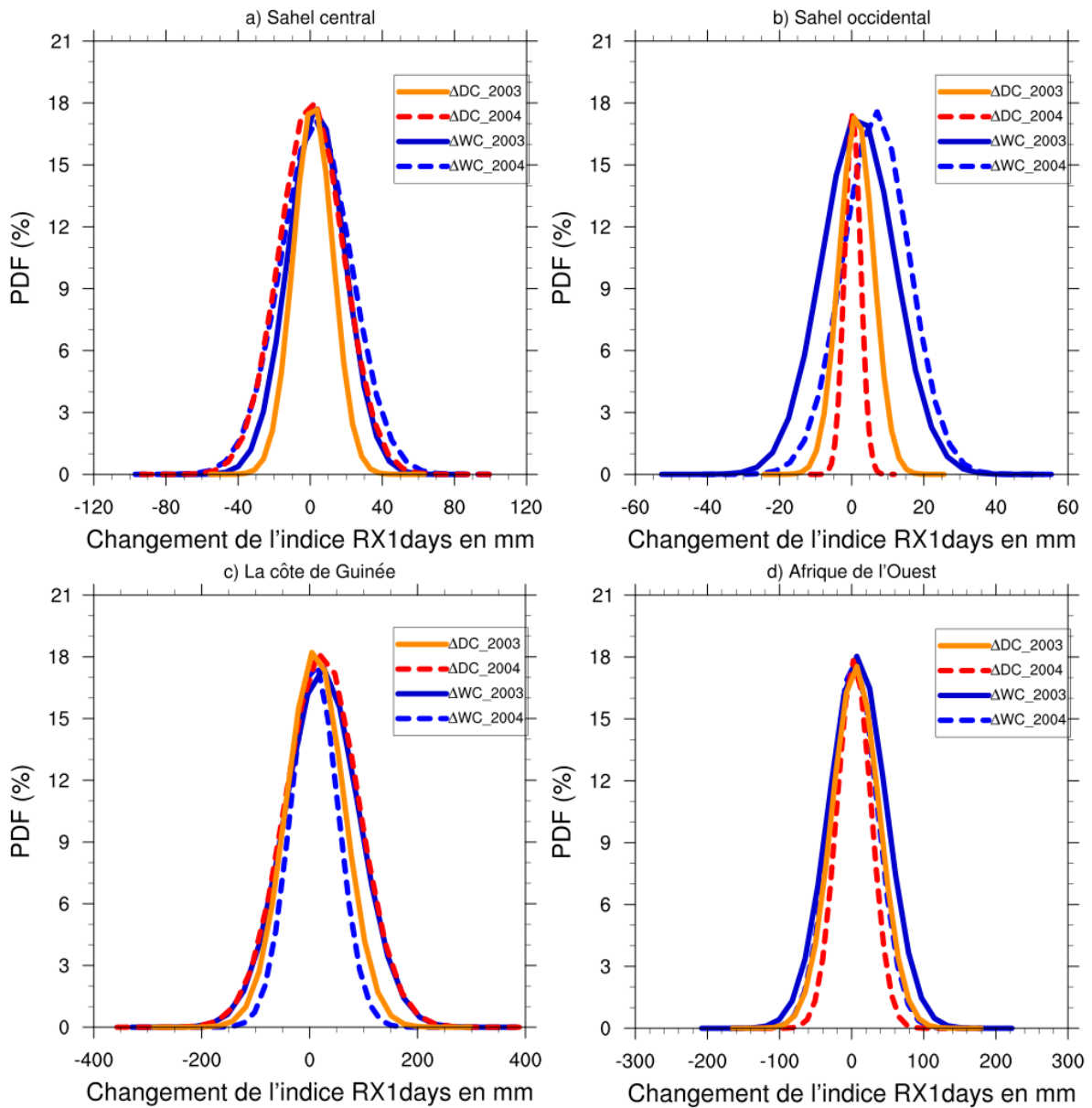
956
957
958
959 **Figure 11**: Same as Fig. 3 but for the RX1DAY index (in mm).
960
961
962
963
964
965
966
967
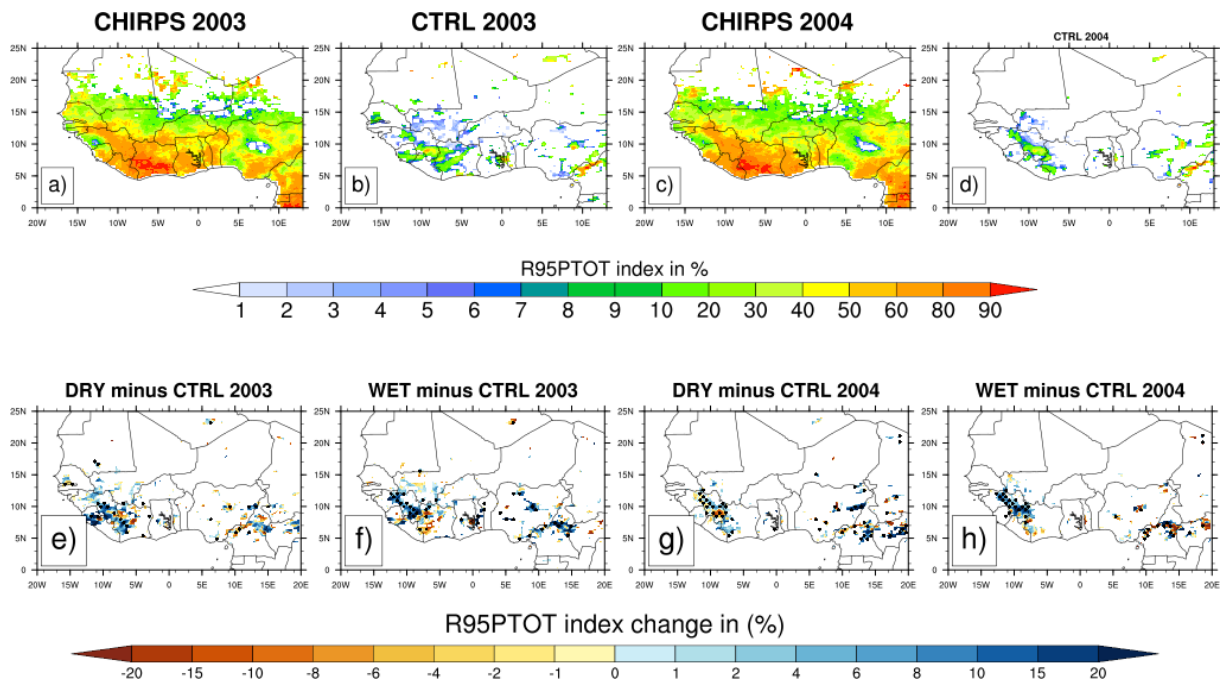
969

970 **Figure 12:** Same as Fig. 2 but for the R95pTOT index (in %).

971

972

973

974

975

976

977

978

979

980

981

982

983

984

985

986

987
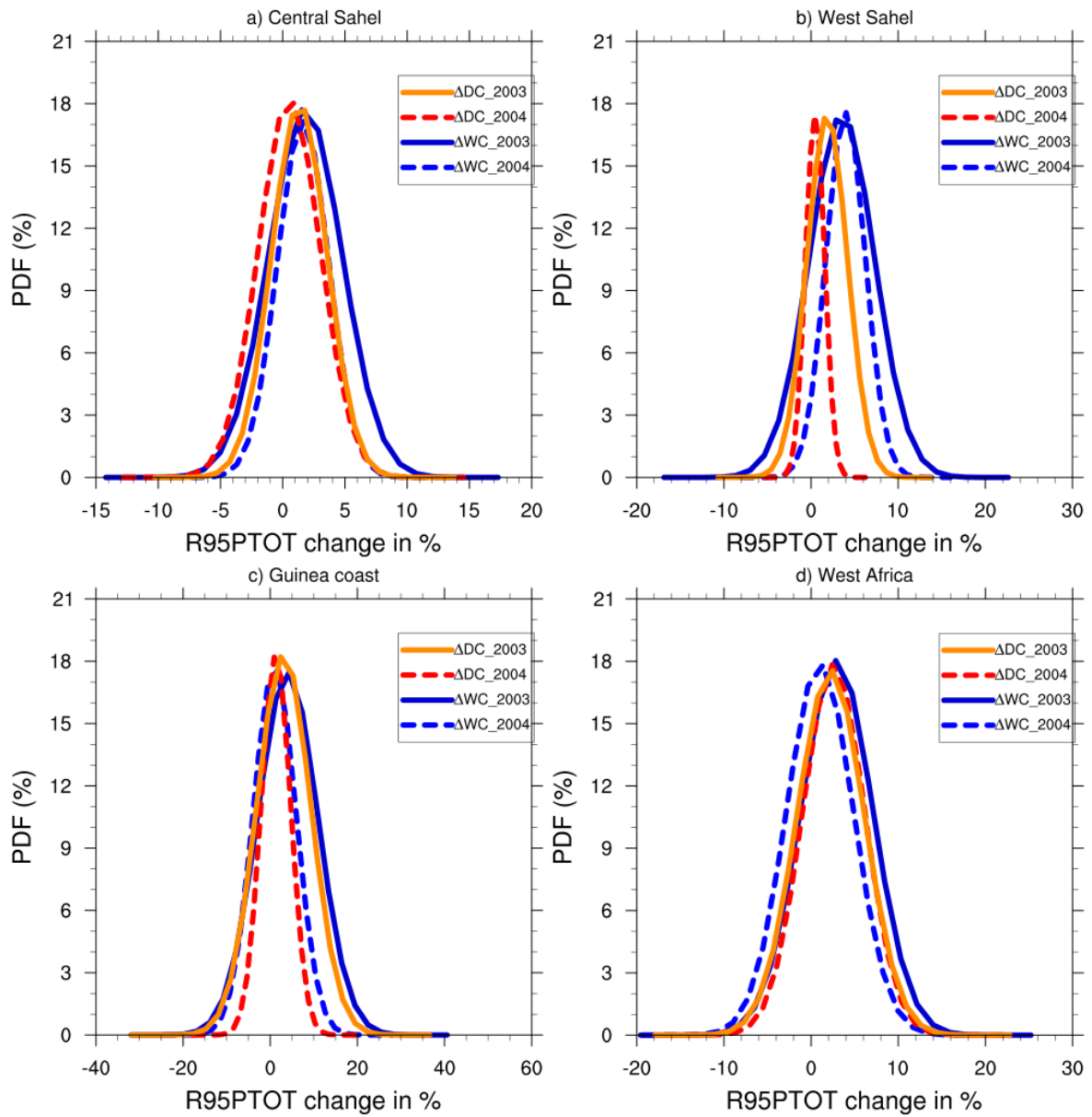
989   **Figure 13:** Same as Fig. 3 but for theR95pTOT index (in %).

990

991

992

993

994

995

996

997

998
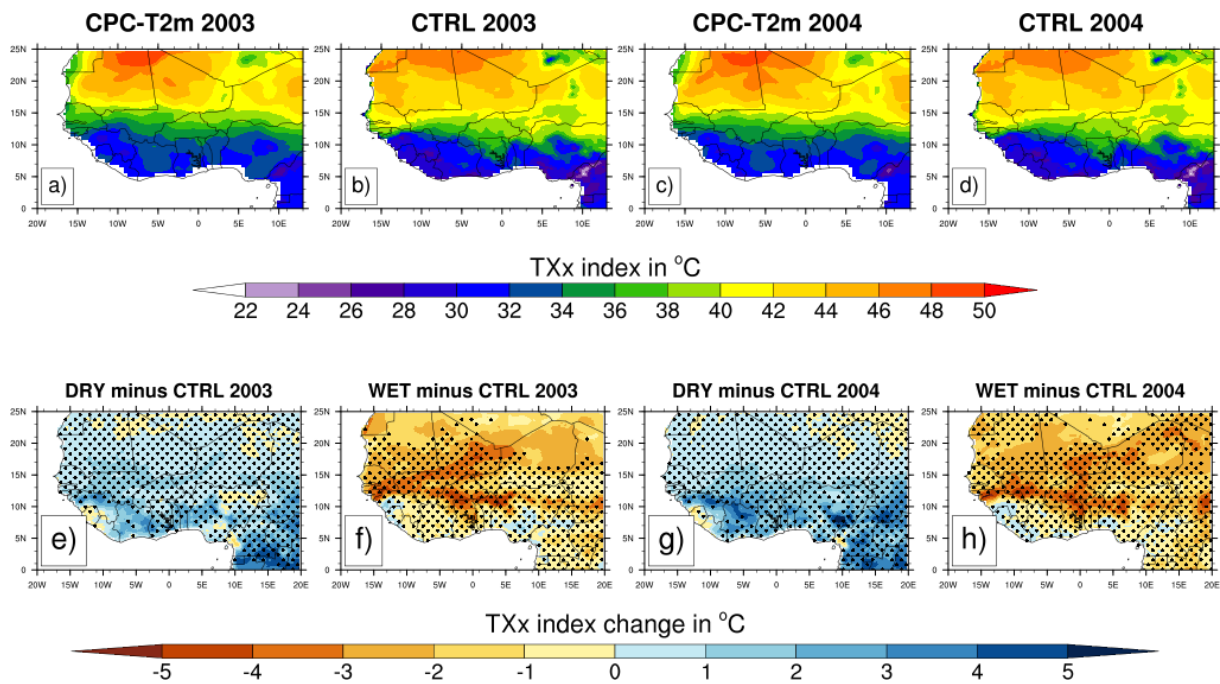
Figure 14: The mean maximum value of daily maximum temperature (TXx index in°C) from CPC-T2m observation (a and c) for JJAS 2003 and JJAS 2004 and the simulated control (CTRL) experiments (b and d) initialized with the initial soil moisture of the ERA20C reanalysis (first panel) and changes in TXx index in°C (second panel) for JJAS 2003 and JJAS 2004, from dry (e and g) and wet (f and h) experiments with respect to the control experiments. Areas with values passing the 95% significance test are dotted.
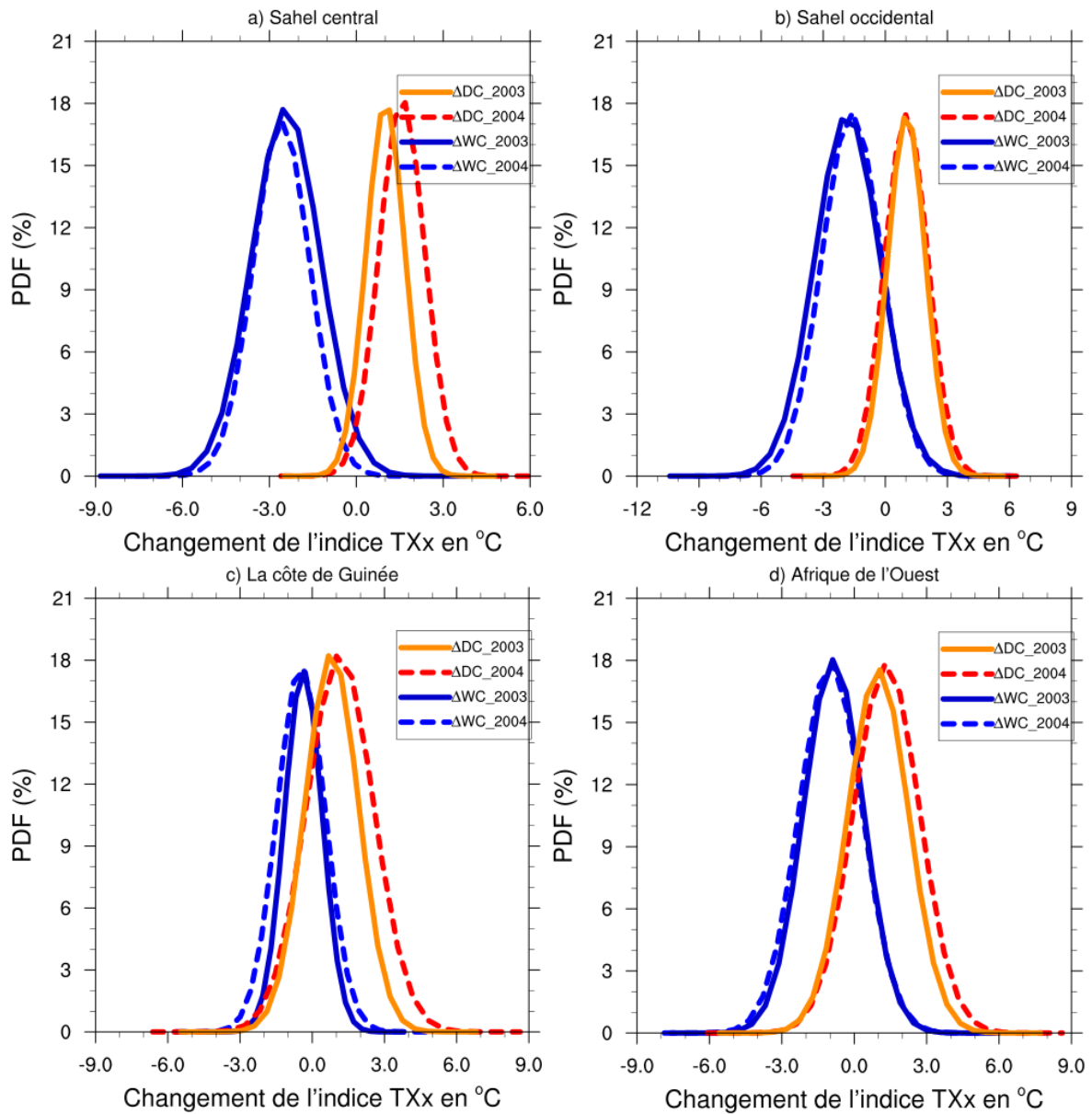
Figure 15: PDF distributions (%) of change in maximum value of daily maximum temperature (TXx index, in°C) for JJAS 2003 and JJAS 2004, over (a) Central Sahel , (b) West Sahel, (c) Guinea and (d) West Africa derived from dry (ΔDC) and wet (ΔWC) experiments compared to the control experiment.
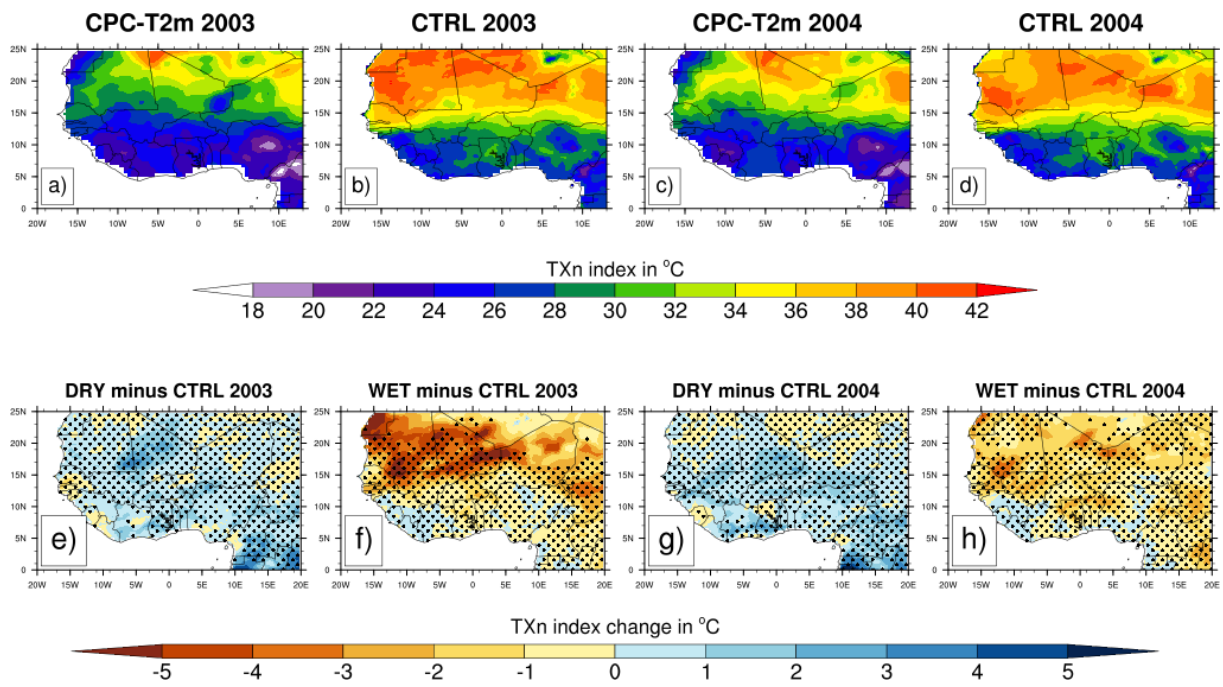
1035

1036

1037 **Figure 16:** Same as Fig. 14 but for the TXn index

1038

1039

1040

1041

1042

1043

1044

1045

1046

1047

1048

1049

1050

1051

1052

1053
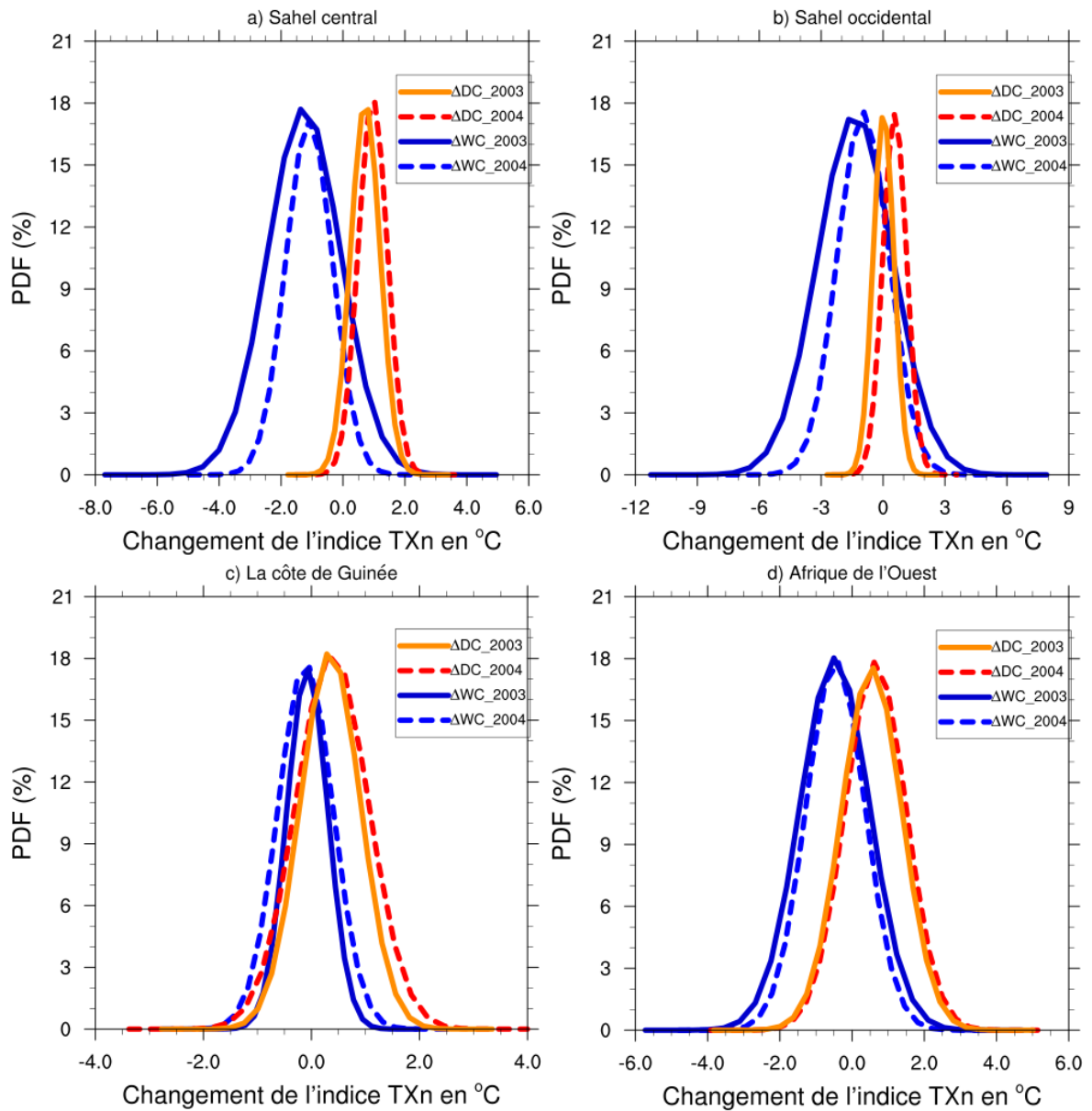
1054

1055

1056

1057

Figure 17: Same as Fig. 15 but for the TXn index.

1059

1060

1061

1062

1063

1064

1065
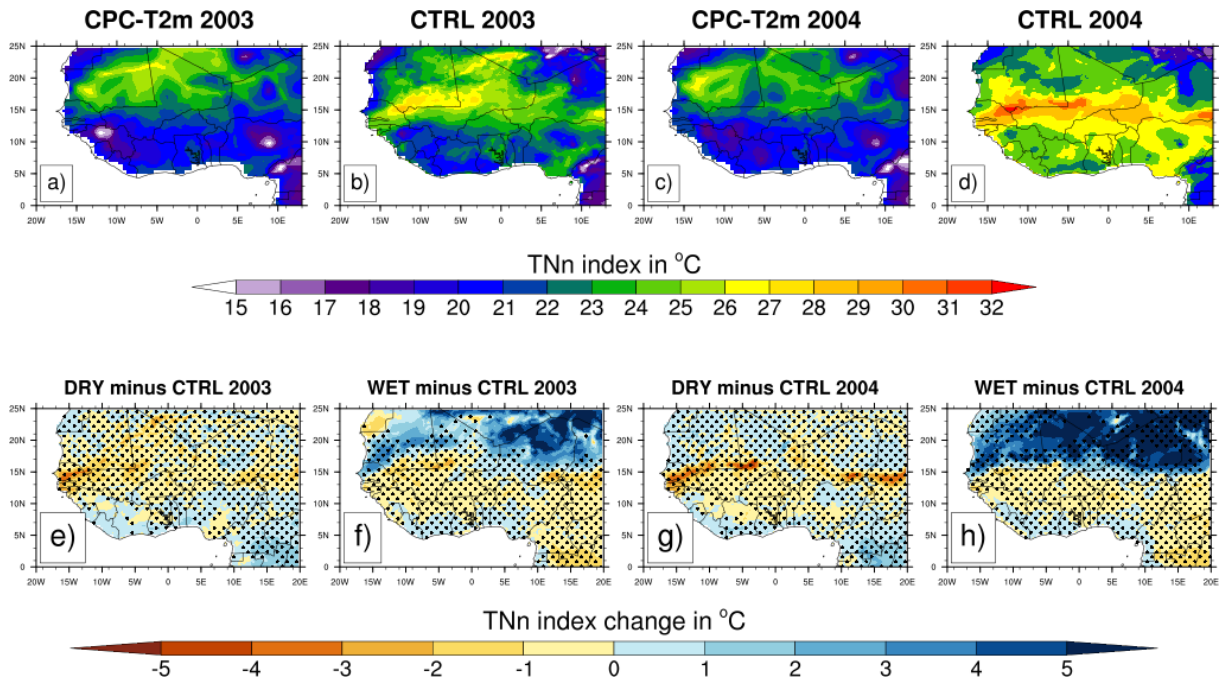
1067

1068

1069   **Figure 18:** Same as Fig. 14 but for the TNn index.

1070

1071

1072

1073

1074

1075

1076

1077

1078

1079

1080

1081

1082

1083

1084
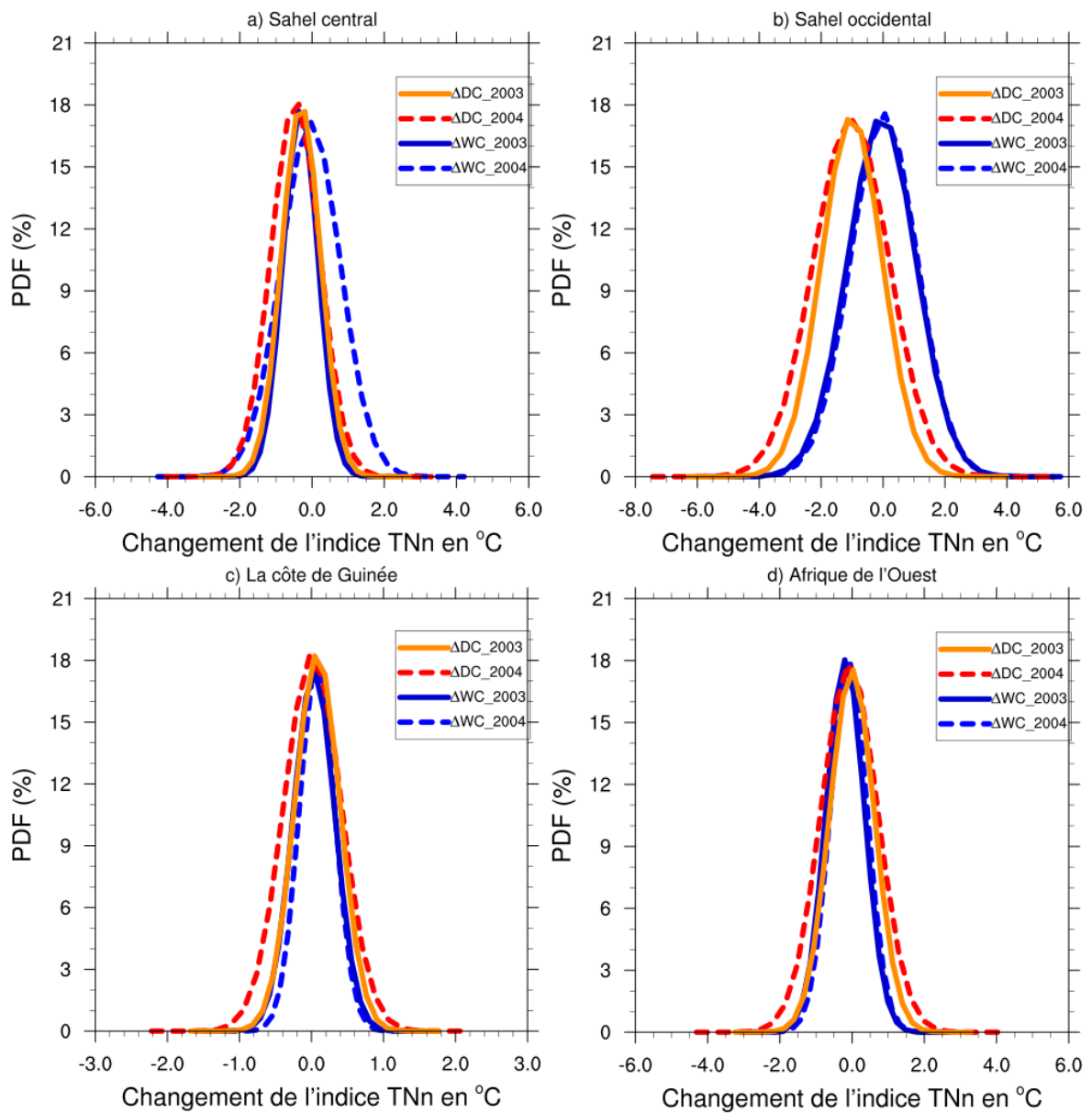
1085
1086
1087
1088

1089   **Figure 19:** Same as Fig. 14 but for the TNn index.

1090
1091
1092
1093
1094
1095
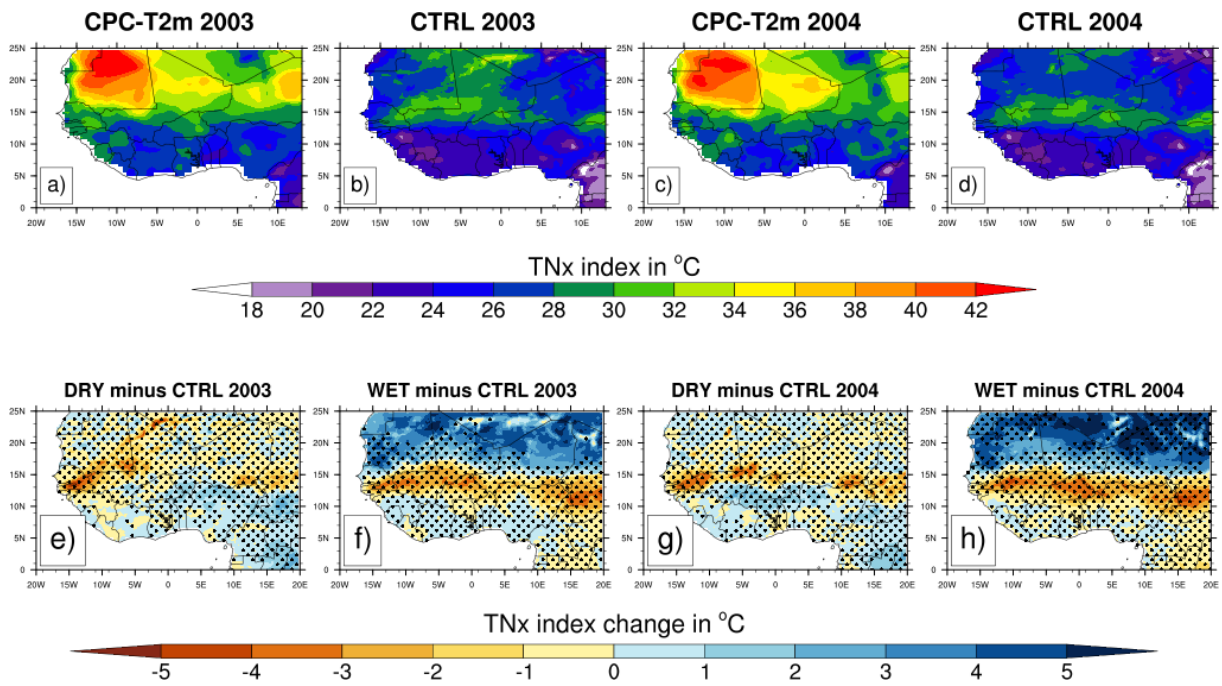
1096

1097

1098

1099 **Figure 20:** Same as Fig. 14 but for the TNx index

1100

1101

1102

1103

1104

1105

1106

1107

1108

1109

1110

1111

1112

1113

1114

1115

1116
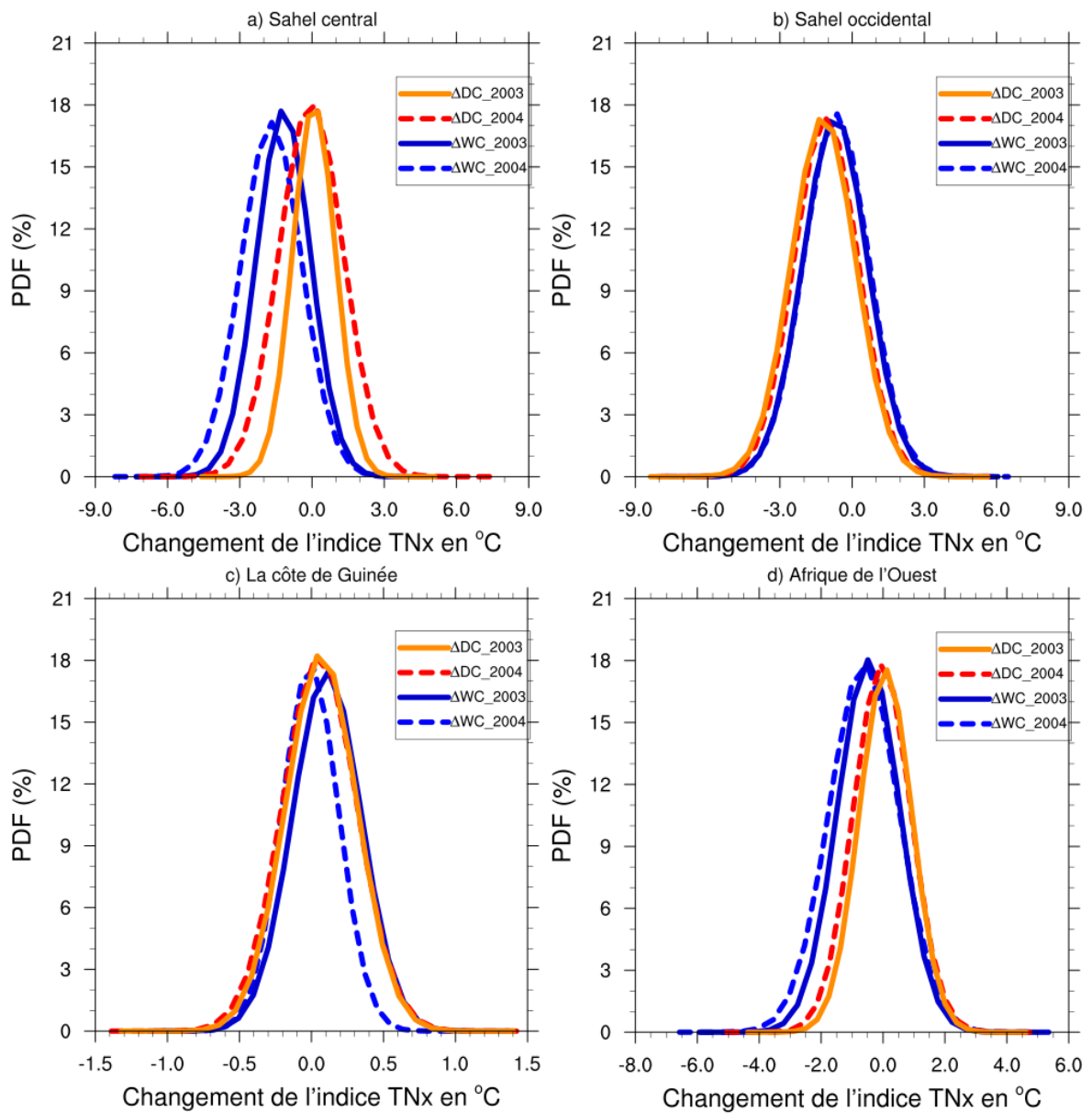
1118

1119 **Figure 21:** Same as Fig. 15 but for the TNx index.

1120